SIGNAL CONTROLLER IN THE LOOP SIMULATION

Final Report

SPR 861

Oregon Department of Transportation

SIGNAL CONTROLLER IN THE LOOP SIMULATION

Final Report
SPR 861

by

David S. Hurwitz, Ph.D., Professor
Hisham Jashami, Ph.D., Assistant Professor (Senior Research)
Logan Scott-Deeter, Ph.D., Post-Doctoral Scholar
Syed Baqir Ul Husnain, Graduate Research Assistant
Oregon State University
101 Kearney Hall
Corvallis, OR 97331

Xiugang Li, Ph.D., P.E.
Oregon Department of Transportation
Research Section

for

Oregon Department of Transportation
Research Section
555 13th Street NE, Suite 1
Salem OR 97301

and

Federal Highway Administration
1200 New Jersey Avenue SE
Washington, DC 20590

March 2026

Technical Report Documentation Page

1. Report No. FHWA-OR-RD-26-08	2. Government Accession No.	3. Recipient's Catalog No.
4. Title and Subtitle Signal Controller in the Loop Simulation		5. Report Date March 2026
		6. Performing Organization Code
7. Author(s) David Hurwitz, 0000-0001-8450-6516 Hisham Jashami, 0000-0002-5511-7543 Logan Scott-Deeter, 0000-0001-5320-0848 Syed Baqir Ul Husnain, 0000-0001-6710-1779 Xiugang Li, 0000-0002-5966-8158		8. Performing Organization Report No.
9. Performing Organization Name and Address Oregon Department of Transportation Research Section 555 13th Street NE Salem, OR 97301		10. Work Unit No. (TRAIS) 11. Contract or Grant No.
12. Sponsoring Agency Name and Address Oregon Dept. of Transportation Research Section 555 13th Street NE, Suite 1 Salem, OR 97301 Federal Highway Admin. 1200 New Jersey Avenue SE Washington, DC 20590		13. Type of Report and Period Covered _____ Report 14. Sponsoring Agency Code
15. Supplementary Notes		

16. Abstract

A novel Hardware-in-the-loop Simulation tool was constructed to show how modifications to signal timings would improve coordinated corridor performance. A total of 15 unique microsimulation models were developed and run three times each to test three case studies of bi-direction bandwidth optimization, cycle length sensitivity, and leading pedestrian interval sensitivity. Results show that optimization can improve overall corridor operation, and that all approaches and turning movements must be evaluated. Specific improvements can be targeted using shorter cycle lengths, but cycle length reaches a point where diminishing returns are experienced. Leading Pedestrian Intervals can provide safety improvements for pedestrians, but the effects are influenced by the optimization strategies.

17. Key Words Signal, VISSIM, Coordinated, Corridor, HILS, Optimized, LPI, Cycle Length, Modeling		18. Distribution Statement Copies available from NTIS, and online at www.oregon.gov/ODOT/TD/TP_RES/	
19. Security Classification (of this report) Unclassified	20. Security Classification (of this page) Unclassified	21. No. of Pages 97	22. Price

SI* (Modern Metric) Conversion Factors
Approximate Conversions to SI Units

Physical Quantity	Symbol	When You Know	Multiply By	To Find	Symbol
Length	n	inches	25.4	millimeters	mm
Length	ft	feet	0.305	meters	m
Length	yd	yards	0.914	meters	m
Length	mi	miles	1.61	kilometers	km
Area	in2	square inches	645.2	square millimeters	mm2
Area	ft2	square feet	0.093	square meters	m2
Area	yd2	square yard	0.836	square meters	m2
Area	ac	acres	0.405	hectares	ha
Area	mi2	square miles	2.59	square kilometers	km2
Volume	fl oz	fluid ounces	29.57	milliliters	mL
Volume	gal	gallons	3.785	liters **	L
Volume	ft3	cubic feet	0.028	cubic meters	m3
Volume	yd3	cubic yards	0.765	cubic meters	m3
Mass	oz	ounces	28.35	grams	g
Mass	lb	pounds	0.454	kilograms	kg
Mass	T	short tons (2000 lb)	0.907	megagrams (or "metric ton")	Mg (or "t")
Temperature (exact degrees)	oF	Fahrenheit	5 (F-32)/9 or (F-32)/1.8	Celsius	oC
Illumination	fc	foot-candles	10.76	lux	lx
Illumination	fl	foot-Lamberts	3.426	candela/m2	cd/m2
Force and Pressure or Stress	lbf	poundforce	4.45	newtons	N
Force and Pressure or Stress	lbf/in2	poundforce per square inch	6.89	kilopascals	kPa

*SI is the symbol for the International System of Measurement
** Volumes greater than 1000 L shall be shown in m^3

SI* (Modern Metric) Conversion Factors
Approximate Conversions from SI Units

Physical Quantity	Symbol	When You Know	Multiply By	To Find	Symbol
Length	mm	millimeters	0.039	inches	in
Length	m	meters	3.28	feet	ft
Length	m	meters	1.09	yards	yd
Length	km	kilometers	0.621	miles	mi
Area	mm2	square millimeters	0.0016	square inches	in2
Area	m2	square meters	10.764	square feet	ft2
Area	m2	square meters	1.195	square yards	yd2
Area	ha	hectares	2.47	acres	ac
Area	km2	square kilometers	0.386	square miles	mi2
Volume	mL	milliliters	0.034	fluid ounces	fl oz
Volume	L	liters	0.264	gallons	gal
Volume	m3	cubic meters	35.314	cubic feet	ft3
Volume	m3	cubic meters	1.307	cubic yards	yd3
Mass	g	grams	0.035	ounces	oz
Mass	kg	kilograms	2.202	pounds	lb
Mass	Mg (or "t")	megagrams (or "metric ton")	1.103	short tons (2000 lb)	T
Temperature (exact degrees)	oC	Celsius	1.8C+32	Fahrenheit	oF
Illumination	lx	lux	0.0929	foot-candles	fc
Illumination	cd/m2	candela/m2	0.2919	foot-Lamberts	fl
Force and Pressure or Stress	N	newtons	0.225	poundforce	lbf
Force and Pressure or Stress	kPa	kilopascals	0.145	poundforce per square inch	lbf/in2

For More Information see: https://www.fhwa.dot.gov/publications/convtabl.cfm

3

ACKNOWLEDGEMENTS

The authors would like to thank the Oregon Department of Transportation Research Section for sponsoring this study, the research coordinator Greg Griffin for expertly facilitating the project, all members of the Technical Advisory Committee (Chris Primm, Roger Boettcher, and Nick Fortey) for their thoughtful review of deliverables, and researchers at the University of Nevada, Reno (Dr. Tian Zong and Dr. Aobo Wang) for their meaningful technical contributions to the development of the hardware-in-the-loop simulation tool.

DISCLAIMER

TABLE OF CONTENTS

LIST OF TABLES

LIST OF FIGURES

1.0 INTRODUCTION

Properly timed traffic signals are crucial to improving traffic operations and throughput along corridors with high vehicular volumes. Refinement of these timings across multiple intersections can provide large vehicle platoons with improved benefits such as reduced number of stops, minimized delay, and cost savings. Adaptive signal controls are one advancement that has helped accomplish this feat, which detect vehicles upstream or downstream of a specific location and use this information to better predict the ideal timing parameter to best accommodate present demand (Koonce & Rodegerdts, 2008). However, such technologies are complex and can require extensive testing and adjustment for each specific use case to realize operational and safety benefits. This becomes especially important when considering fluctuations in vehicle loading and travel patterns that arise over time. Drastic changes in these aspects may require retiming or adjustments to be made; These can be done in the field but present the risk of uncertain outcomes and additional cost expenditures. As an alternative option, simulation modeling has been noted to be an efficient avenue for reviewing signal timings and testing potential countermeasures (Koonce & Rodegerdts, 2008). One consideration when selecting this alternative is that more advanced signal controller operations may not be readily available within the default simulation platform (Hunter et. al. 2010; Stevanovic et. al., 2009). A work-around solution to this limiting factor is designing a signal-controller-in-the-loop simulation that leverages input from one or multiple physical signal controllers within the microsimulation environment (Wang et. al., 2019). This is one example of hardware-in-the-loop simulation (HILS), in which the device is used as an intermediary piece of equipment that can be manipulated and adjusted to meet the needs of the desired testing. In addition to providing flexibility for different use cases, multiple microsimulation designs can be created for various corridors so long as the number of physical controllers in the HILS matches that of the referenced location, allowing for corridors of varying lengths to be considered. Longer corridors may be easier to optimize because of the allowable spacing between intersections, while it is believed that shorter corridors may present more difficulty due to the potential for more frequent stops and restrictions between intersections. For this reason, the present study focused on a reference corridor that was shorter and spanned 0.93 miles across 5 signalized intersections in Scappoose, OR.

PTV VISSIM was selected as the preferred microsimulation platform and offered a fully functional traffic signal emulator and a full NTCIP-compliant communication module (Li & Mirchandani, 2016). Additionally, PTV VISSIM was found to feature flexible configurability with the ability to manipulate, code, and control many factors while simultaneously producing a wide variety of performance measures. One consideration when designing a signal-controller-in-the-loop study is that simulation analysis must be run in real-time, given the restriction that the physical signal controllers are influencing timing and detector calls. This becomes an important aspect when studying multiple models, as each configuration takes additional time to complete a full simulation run. In the case of the present study, AM- and PM-peak periods were selected as the primary considerations, with calibration procedures and desired adjustments being made accordingly.

2.0 LITERATURE REVIEW

2.1 TYPES OF IN-THE-LOOP SIMULATION

According to Wang et al. (2021), there are four types of "In-the-Loop" simulation: Emulator-in-the-Loop (EILS), Hardware-in-the-Loop (HILS), Software-in-the-Loop (SILS), and Virtual Controller Interface Device (VCID)-Based HILS. This characterization is described in Table 1, and the types of simulation are described in more detail in the following subsections. Other authors characterize the fourth category as "System-in-the-Loop" simulation, which refers to Advanced Traffic Management Systems (ATMS) (Li & Mirchandani, 2016).

Table 1. EILS, HILS, SILS and VCID-Based HILS (from Wang et al., 2021)

Criteria	Emulator-in the-Loop-Simulation (EILS)	Hardware-in-the Loop-Simulation (HILS)	Software-in-the-Loop Simulation (SILS)	Virtual Controller Interface Device (VCID)-Based HILS
Signal Provider	Controller Emulator	Physical Controller	Virtual Controller	Physical Controller
Traffic Flow	Traffic Simulation	Traffic Simulation	Traffic Simulation	Traffic Simulation
Connection	Wireless	SDLC/RS232/RS 485	Wireless	Ethernet

2.1.1 Emulator-in-the-Loop Simulation (EILS)

Emulator-in-the-Loop simulation is described by Wang et al. (2021) as the simplest of the four simulation methods described in Table 1. This type of simulation performs all components of the modeling and evaluation process of the traffic signal controller and its parameters using a built-in controller within the simulation software. Examples of common EILS-capable software include CORSIM, SimTraffic, VISSIM, AIMSUN, and TransModeler (Li & Mirchandani, 2016; Wang et al., 2021). Because EILS does not involve interfacing the simulation platform with any physical hardware, it is typically faster to process and more cost-effective than the other simulation options. However, these systems are limited in their ability to model more advanced traffic signal control strategies, like adaptive or coordinated signal systems. Furthermore, the algorithms for signal control may operate in a black-box, meaning the EILS user may not receive the necessary insight into the emulated controller's operations. (Wang et al., 2021).

2.1.2 Software-in-the-Loop Simulation (SILS)

Software-in-the-Loop simulation is an extension of HILS which operates entirely virtually: it uses a virtual traffic controller, separate from the traffic simulation platform, in place of a real traffic controller. A virtual interface transfers data between the simulation platform and the

virtual traffic controller. This method can be used if the virtual representation of the traffic controller, the "software", is considered a reliable-enough representation of the real traffic controller (Wang et al., 2021). SILS requires either the development of the virtual traffic controller or selection of a pre-developed virtual traffic controller. This can pose several challenges. Even when provided all the necessary information, development of a virtual traffic controller can be time-prohibitive, and the release of new controller versions or software updates will necessitate continuing development. Virtual controller development requires that control logic is not proprietary (Wang et al., 2021).

2.1.3 Traffic Signal Controller HILS

HILS has been shown to be more effective at simulating real-world traffic conditions and allows for analysis of a broader range of traffic signal controllers as compared to similar alternatives (Engelbrecht, 2001; Wang et al., 2021). HILS includes three key components: 1) a microsimulation platform; 2) the controller interface device (CID); and 3) the traffic signal controller. The CID bridges the connection between the microsimulation platform and the physical traffic signal controller, shown in Figure 1. One CID is required per traffic signal controller (Wang et al., 2021).

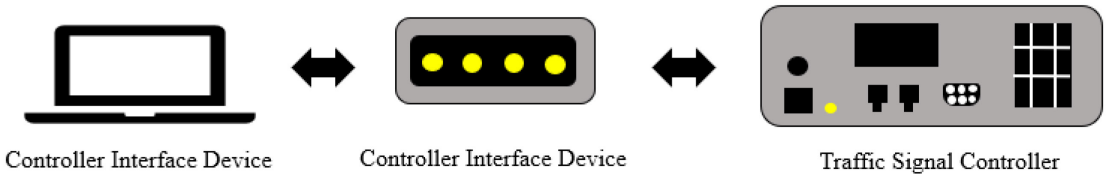

Figure 1. Physical Architecture of HILS

The simulation platform manages detector input data from simulated vehicles, which is transmitted to the real traffic controller via the CID. The physical traffic controller is then able to receive the detector input and determine the signal status based on the programmed phasing parameters, which is then returned to the signal within the simulation model via the CID (Wang et al., 2021). This data exchange process repeats at every simulation time step (Stevanovic et. al., 2009). The logical architecture of HILS is described in Figure 2.

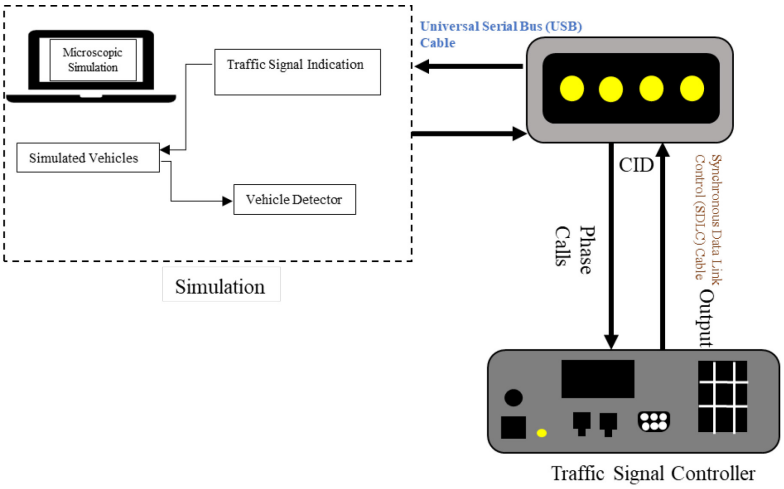

Figure 2. Logical Architecture of HILS

HILS has been used successfully in prior work to evaluate signal performance prior to deployment in the field under a variety of use cases. Koonce et al. in 1999 used HILS to evaluate traffic signals at diamond interchanges, which are vulnerable to inefficient traffic flow, and found HILS measured signal performance accurately, compared to other field-based engineering studies (Koonce et. al., 1999). Byrne et al. in 2005 used HILS to successfully evaluate the effect of near- and far-side bus stop locations on transit signal priority in Portland, OR (Byrne et. al., 2005). Abadi et al. in 2019 applied HILS to evaluate alternative red clearance extension system designs using the microsimulation platform PTV VISSIM and a 2070 ATC controller, connected through a NIATT-produced CID (Abadi et al., 2019). Additional studies have used HILS to compare manual versus optimized traffic signal control in oversaturated conditions and intersection signal timing strategies with respect to multimodal delay (Marnell et al., 2017). In this case, HILS and software-in-the-loop systems were deployed as a necessary method to accommodate complex transit operations within the proposed intersection using the built-in PTV VISSIM signal controller functionality.

HILS has also been used to assess coordinated and adaptive signal systems. Abdelgawad et al. in 2015 compared optimized and coordinated actuated signal timing plans with a novel self-learning Adaptive Traffic Signal Control (ATSC) system, MARLIN-ATSC, using HILS and an ATC-1000 Traffic Controller from PEEK and the Paramics microsimulation platform. The simulation results suggested the system's potential to reduce intersection delay by up to 20% (Abdelgawad et al., 2015). Yun et al. in 2007 used HILS with an EPAC 300 traffic CID and the PTV VISSIM microsimulation platform to evaluate the potential of an adaptive maximum green signal parameter, in which the signal controller could adjust maximum green intervals according to the degree of traffic demand and fluctuations. Using average delay and average number of stops as performance measures, the HILS-derived data suggested the adaptive maximum green outperformed the typical maximum green (Yun et al., 2007).

However, HILS may not always be a feasible simulation method due to several limitations. First, it runs in real time and must be processed by a system that can do the same (Engelbrecht, 2001). Because of the need to synchronize the simulation speed with the signal controller, simulating many scenarios can take a long time (Li & Mirchandani, 2016). Second, the requirement that

every signal controller must be paired with its own CID can increase cost in scenarios where multiple traffic signals are being tested in tandem. Third, the serial cables required by the CIDs to interface the simulation platform with the real traffic controller can temporarily disconnect, causing errors in the experimental data or the system to crash. Because of this, the system may not be advisable for lengthy simulations (Wang et al., 2021).

2.1.4 Virtual Controller Interface Device (VCID)-Based HILS

Virtual Controller Interface Device-based HILS, proposed by Wang et al. (2021), is a novel concept which addresses the cost and communication reliability limitations posed by HILS. It connects real traffic signal controllers with simulation software wirelessly using the National Transportation Communications for ITS Protocol (NTCIP) and allows the user to update, in real time, signal controller parameters while running the simulation. Wang et al. (2021)'s system used VISSIM to interface with Econolite Cobalt controllers. A key limitation of the VCID-based HILS is that it can currently only accommodate the Econolite controllers applied in the Wang et al. (2021) case study, as NTCIP protocol does not currently allow VISSIM to transmit direct detector input to a physical controller out of safety concerns related to malicious intention which has been said to have the potential to break down traffic flow (Wang et. al., 2021). Wang et al. (2021) anticipate that this issue will be resolved in the next NTCIP version. To resolve this problem, (Wang, Tian, Gholami, et al., 2021) collaborated with Econolite Group, which provided them software code and made them able to place external detector calls possible.

Development of a robust VCID required the consideration of several design elements. Packet losses and data transfer errors must be accounted for. As such, it is necessary to design a reliable processing technology to avoid these errors. To model complex traffic signal systems, a mapping of traffic signal display and detector calls to the controllers and simulation software package is required. During the simulation process, a large amount of data is exchanged. For real-time simulation applications, a data processing frequency of 10 Hz is required, both for the controllers and the microsimulation environment. When the communication bandwidth is narrow, the threads of the VCID should also be synchronized. Finally, in multi-threaded programming, special attention must be paid to memory operation and thread stability to avoid memory leaks and thread loss. The data flows for VCID are given in Figure 3.

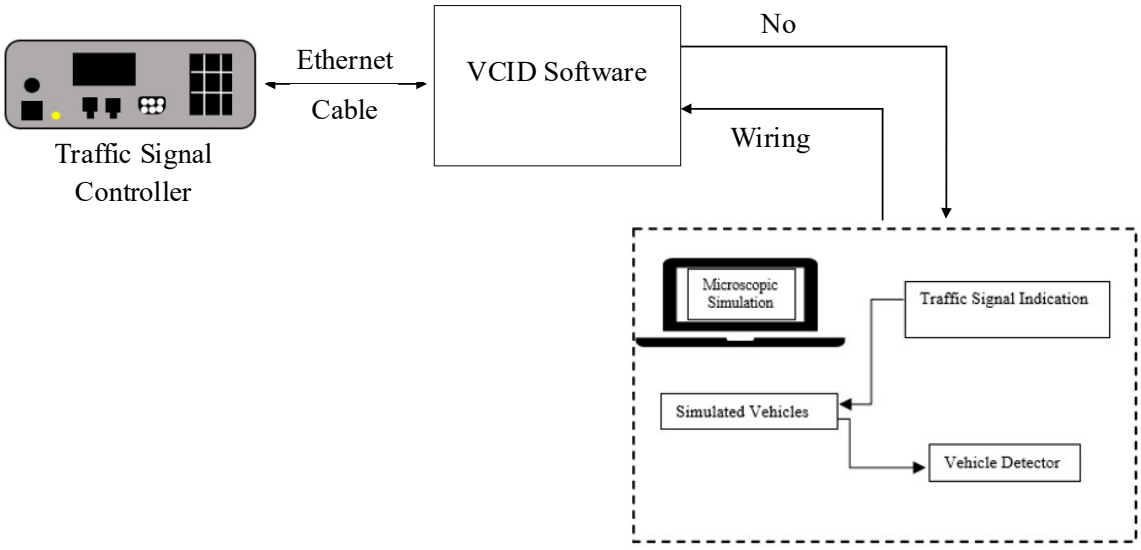

Figure 3. Structure of VCID based HILS

VCID supports real-time data communication between physical signal controllers and traffic simulation software. The controlled experimental results between SILS and VCID show that the function of the VCID is very similar to SILS, with a 1.8% difference between the two systems. The performance of SILS and VCID can be considered statistically indifferentiable. However, the development cost of SILS is comparatively high, which is one of its biggest disadvantages alongside requiring signal controller manufacturers to make their code public. A comparison between SILS and VCID is shown in Table 2. When simulating different signal phasing and timing plans, VCID simulation results are closer to real-world traffic conditions. Although the VCID has some limitations including a lack of time synchronization between the actual signal controllers and the simulation software, it has the potential to produce accurate and reliable simulation results.

Table 2. Characteristics comparison between SILS and VCID

Characteristics	SILS	VCID
Development and maintenance costs	High	Low
Device cost	Low	High
Running cost	Low	Low
Data processing cost	High	Low
Stability	High	High
Real-world traffic operational conditions	No	Yes
Online debugging	No	Yes
Time synchronization issue	No	Yes

2.2 COMPARISON OF SIMULATION CONCEPTS

Wang et al. (2021) compared HILS, SILS, EILS, and VCID-based HILS and found that all systems generally produced similar performance measures (Wang et al., 2021). Stevanovic et al.

(2009) compared HILS, SILS, and EILS in an evaluation of five scenarios using the VISSIM microsimulation platform. The following variables and variable levels were considered:

- Network size: one to five intersections
- Operational strategies: pretimed, actuated, actuated-coordinated, and two signal transition logics

All three simulation strategies performed similarly for "basic signal control operations, such as pretimed and isolated actuated operations". However, EILS produced "significantly different" outcomes than the HILS and SILS strategies when "advanced controller operations were used, such as signal transition logic" (Stevanovic et al., 2009b). EILS, works on a 1-Hz controller frequency as compared to SILS and HILS, which work on 10 Hz controller frequencies. In free-running operations the consequences of this frequency differential caused slightly worse performance for the EILS.

Chowdhury et al. (2018) compared the performance of five HILS and five SILS signal control platforms for a single intersection and the same signal timing plan using VISSIM. The five HILS controllers were: Econolite (Cobalt), Intelight (2070-LDX), McCain (ATC eX), PEEK (ATC-1000), and Siemens (m50). The five SILS controllers were: ASC/3 Econolite, Fourth Dimension (Virtual D4), McCain 2033, Ring-Barrier Controller, and Siemens Virtual Next Phase. The study found that each signal control platform performed relatively consistently, however, there were large enough differences between the HILS and SILS results that "it cannot be claimed that use of any of these platforms will result in signal timings identical, or very similar, to another platform" (Chowdhury et al., 2018).

Marnell et al. (2017) compared two intersection signal phasing scenarios utilizing HILS and SILS in tandem with the VISSIM microsimulation modeling platform. Unlike using HILS, the SILs strategy allowed the users to run the simulation faster than real time. However, information flow was similar for both simulation strategies and produced useful data on average delay for both phasing scenarios analyzed (Marnell et al., 2017).

2.3 STATE OF PRACTICE

2.3.1 Microsimulation Modeling Platforms

Common to all "In-the-Loop" simulations is the decision of what simulation platform should be used. Any modeling platform must be calibrated to the specific traffic scenarios the user desires to test—for example, peak hour traffic flow (Li & Mirchandani, 2016). Historically, CORSIM, VISSIM, and SimTraffic software are examples of microsimulation platforms which have supported assessment of traffic control strategies (Engelbrecht, 2001). Table 4 presents examples of simulation platforms used in recent studies. Among the studies reviewed for this literature review, VISSIM was the most commonly-used microsimulation modeling platform, and is arguably also one of the more commonly-used microsimulation modeling platforms in industry. It contains both a fully-functional traffic signal emulator and a full NTCIP-compliant communication module (Li & Mirchandani, 2016).

Table 3. "In-the-Loop" Simulation Platforms for Example Studies

Simulation Platform	Example
VISSIM	Abadi et al., 2019; Chowdhury et al., 2018; Li & Mirchandani, 2016; Marnell et al., 2017; So et al., 2013; Stevanovic et al., 2009; Yun et al., 2007
Paramics	Abdelgawad et al., 2015

2.3.2 Testing of Signal Timings

Signal timers commonly use a suitcase controller tester to evaluate signal timing in advance of field implementation. The following picture shows an example of the controller tester. Signal timing is input into the traffic signal controller software, such as MaxTime, ODOT's current standard. The suitcase controller tester is connected to a traffic signal controller. Signal timers manually activate a signal phase to test if the signal phases run as expected. In addition, signal timers input the signal timing into the controller, put the controller into the cabinet in the lab, and connect the controller to the conflict monitor to test the signal timing. In this testing procedure, signal timing parameters are not evaluated against real traffic conditions. This project will improve the testing procedure options available to ODOT by using controller-in-loop simulation to match the signal timing parameters with real traffic conditions.

Figure 4. Example of a Controller Tester

2.3.3 Testing New Traffic Signal Controller Software

Vendors update traffic signal controller software regularly. New versions of controller software, such as MaxTime, require testing before receiving approval for ODOT's statewide implementation. Signal timers install new versions of software and signal timing on a controller and use the suitcase controller tester to evaluate the new controller software by manually activating signal phases. ODOT has procedures in place for using certain simulation tools for assessing signalized intersections, with templates readily accessible for Synchro/SimTraffic (ODOT, 2025). These packages allow users to create models, optimize traffic signals, and perform capacity analysis to test new signal controller timing or implementation (Jones et. al., 2004). Often, the simulation software installed on a laptop connects to the controller via a CID, which permits communication and allows the simulation software to generate actuations of the traditional eight signal phases that help test the new controller software. Furthermore, new

versions of adaptive software, such as Maxadapt, cannot be tested in the lab because the testing needs to connect the traffic simulation software to multiple controllers. This research project used the commercial traffic simulation software, VISSIM, to test the new controller capabilities.

2.3.4 Testing Adaptive Signal Control Before Deployment

Adaptive signal control has been deployed on highway corridors in Oregon, and there is increasing interest by the agency in adopting this control strategy on additional corridors. Currently, ODOT cannot use simulations to compare traffic signal performance quantitatively before deploying adaptive control in the field. Signal timers may find that adaptive control does not improve traffic performance until it is deployed in the field, resulting in wasted agency resources (e.g., time and money). This project proposes to use controller-in-loop simulation to connect multiple controllers and compare the traffic performance before deploying the adaptive control. This will increase the likelihood that the investment in adaptive control results in better traffic performance.

2.3.5 Automated Traffic Signal Performance Measures

ODOT has adopted automated traffic signal performance measures (ATSPM). ATSPM data can be used to improve the signal retiming process and provide continuous evaluation of performance based on observable field conditions (FHWA, 2020). These performance measures have been used to identify challenges experienced in the field (i.e., excessive transition times, phases being skipped) but in some cases the root causes were not able to be discerned from the ATSPM data alone. Controller-in-the-loop simulation has the potential to more accurately replicate field observed performance for signal timers in the lab so that the cause of atypical or unanticipated traffic performance can be determined, and solutions can be developed. Solutions may include other technology additions or operational strategies, with the FHWA noting adaptive signal control as one alternative to addressing difficult to interpret ATSPM results (FHWA, 2020). A robust controller-in-the-loop simulation can identify how traffic will respond to countermeasures such as adaptive signal controls.

2.4 STRATEGIES FOR EVALUATING PERFORMANCE

A variety of performance measures, often in combination with each other, have been used to evaluate signal controller performance in traffic simulation environments. Commonly cited measures and examples of studies that have used them are shown in Table 4. From this table, the most common measures of effectiveness include average vehicle delay or total delay followed by the number of vehicular stops.

Table 4. Traffic Signal Controller Performance Measures

Performance Measure	Example
Delay	Abdelgawad et al., 2015; Chowdhury et al., 2018; Fayazi et al., 2019; Li & Mirchandani, 2016; Marnell et al., 2017; Stevanovic et al., 2009; Yun et al., 2007
Number of vehicle stops	Chowdhury et al., 2018; Fayazi et al., 2019; Li & Mirchandani, 2016; Stevanovic et al., 2009; Yun et al., 2007
Travel time	Fayazi et al., 2019; Li & Mirchandani, 2016; Stevanovic et al., 2009
Vehicle trajectory	Fayazi et al., 2019
Queue length	Li & Mirchandani, 2016
Volume/Capacity (v/c) Ratio	Li & Mirchandani, 2016
Average green time allocation	Stevanovic et al., 2009
Average speed	Stevanovic et al., 2009

3.0 EXPERIMENTAL EQUIPMENT

3.1 SOFTWARE PACKAGES

The various software platforms that were used and their primary function within the HILS are described in this section.

3.1.1 MAXTIME

MAXTIME is a software package that allows users to control and manage specific signal controller units via the Q-Free User Interface (UI). With the use of a web browser and the static IP address assigned to the controller of interest, users can monitor functionality and input parameter values such as gap out or maximum/minimum green time. To integrate MAXTIME into the HILS, no unique hardware was necessary. Instead, software was installed on a desktop computer, and a valid account was created that permitted access to the five signal controllers within the same network as the desktop computer being used. This platform provides an easy to interpret visualization for which signal phase is currently timing among other timing related details. Figure 5 shows a screen-capture of the MAXTIME UI. From visual inspection of this image, one can observe the timing at US30 & High School Way-Walnut Street, that signal phases 2 and 6 are currently displaying a green signal while phases 1, 4, 5, and 8 are given a red signal indication. Additionally, calls have been placed for queued traffic along phases 2 and 6. This information was compared in real-time with the simulation model to ensure the controller and simulation are well synchronized.

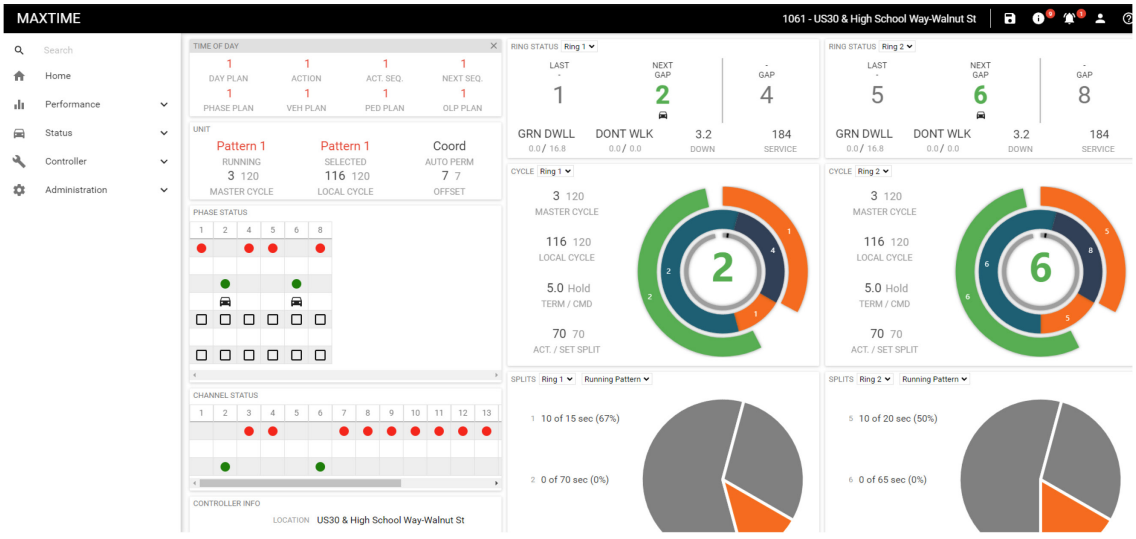

Figure 5. Example MAXTIME Interface

3.1.2 PASS

The software that performs a bridging function between PTV VISSIM and the signal controllers is PASS, which decodes information from both sources and relays the information between platforms. PASS is composed of a UI that provides a visual interpretation of signal timing and coordination across a corridor, but communicates via a Virtual Controller Interface Device (VCID) Script. The VCID is a text file containing lines of commands interpretable by PTV VISSIM. This script also houses the IP addresses of all signal controllers. The VCID dictates what is displayed on the PASS UI, the primary interface that a user may interact with as it provides visual representations of system functionality. An example of part of the VCID script is shown in Figure 6a, while Figure 6b describes the associated timing plans and visual presentation of the study corridor.

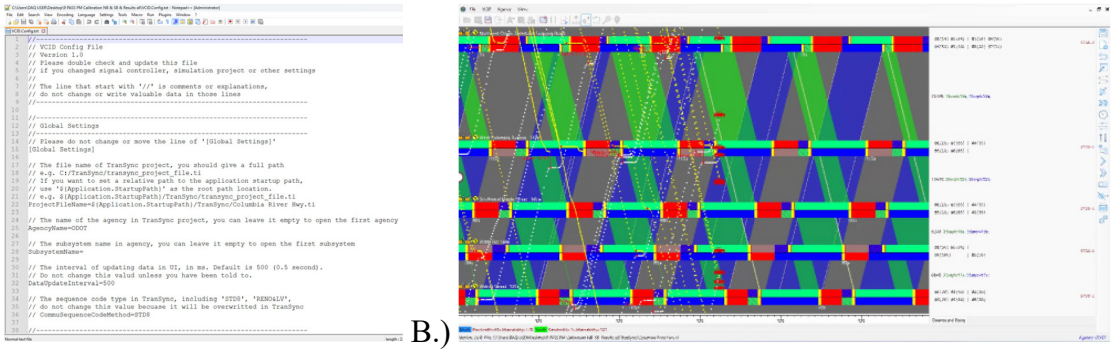

B.)

Figure 6. Example A.) VCID Script and B.) PASS UI

Figure 6b shows the PASS UI, specifically the signal timing plans and traffic flow along the corridor. Time is displayed on the horizontal axis while distance is represented on the vertical axis. The signal phases at the intersections of interest run horizontally across the screen and act as a separator for the roadway segments along the vertical axis. The blue blocks (i.e., sections running diagonally from the bottom-left to the top-right) describe the coordinated bands of traffic flow in the Northbound direction. From this example, the blue bands are synced to allow at least some vehicles traveling at the progression speed to consistently navigate the corridor without significant stopping. Alternatively, the coordination indicated by the green bands (i.e., sections running from top-left to bottom-right), is not as successful. These observations indicate that if the Northbound vs. Southbound directions of flow were to be compared, the Northbound would prove to be more efficient under the current timing pattern.

3.1.3 PTV VISSIM

A PTV VISSIM model was constructed that resembled the field location of interest. The base PTV VISSIM model was developed independent of the other software packages and used signal timings alongside Turning Movement Counts (TMC) to generate a representative model of the field study site described in Section 4.2. Calibration procedures were performed in accordance with the ODOT Protocols for PTV VISSIM Simulation and ensured an adequate warm-up and cool-down time of 30-minutes to allow traffic to reach representative levels (ODOT, 2011). Figure 7 shows a screen capture of this model.

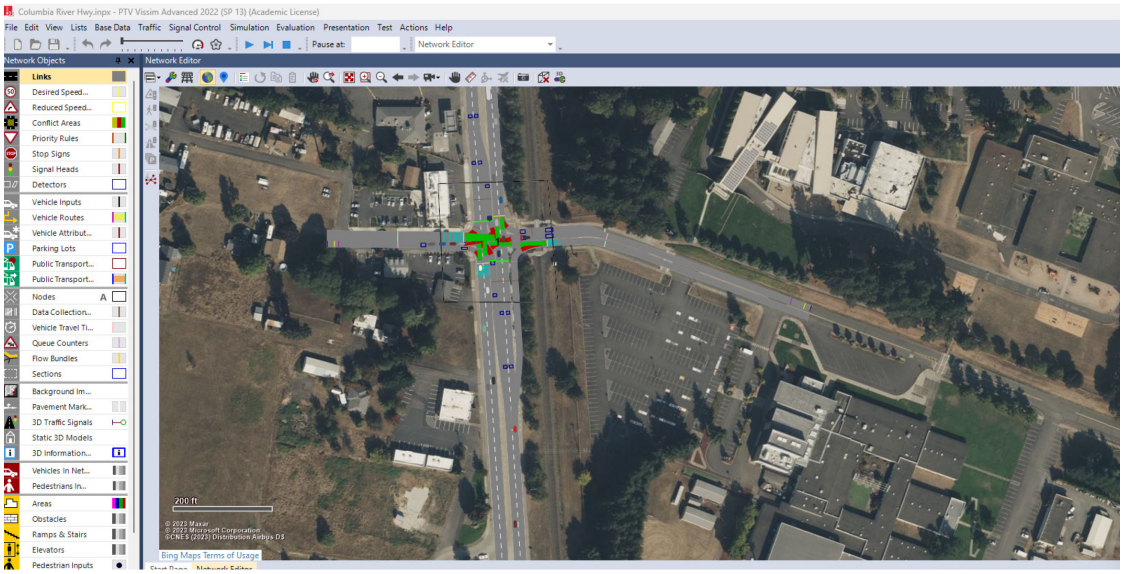

Figure 7. Example PTV VISSIM Model of US30 at Walnut Street

3.1.4 WaySync

WaySync software provided a tool for coding new signal phasing and timing into the PASS system, producing new optimizations along the corridor, and as assessing the performance of the coordinated signal system. Two versions of WaySync, WaySync-D and WaySync-M, were used.

WaySync-D is an abbreviation for WaySync-Desktop, which was installed on the same desktop computer with all other software packages used. This application allowed for the management and optimization of the corridor to be carried out, which included manipulation within the various models to achieve the desired cycle lengths and optimization strategies. The configurability of each model was made possible using WaySync-D so that changes in the cycle length across the corridor could be made or individual adjustments at an individual traffic signal. Performance output was also provided using the WaySync-D platform, some of which included vehicle trajectories and the results of the corridor synchronization performance index.

WaySync-M, an abbreviation of WaySync-Mobile, is the software package that allowed for real-time evaluation of traffic signal controllers in the field. The availability of this software to be installed on portable devices combined with geo-referencing capabilities allowed for the microsimulation timings created using WaySync-D to be transported into the field and compared with as-built conditions. WaySync-M produced a live time-space diagram (TSD) of vehicle trajectory combined with the simulated model, which was leveraged to understand and diagnose any observed discrepancies. Figure 8 shows the WaySync-M platform during a field trial, which used the front-facing camera on a seventh-generation iPad Pro to collect a video feed alongside the vehicle trajectory within the TSD at the field corridor of interest.

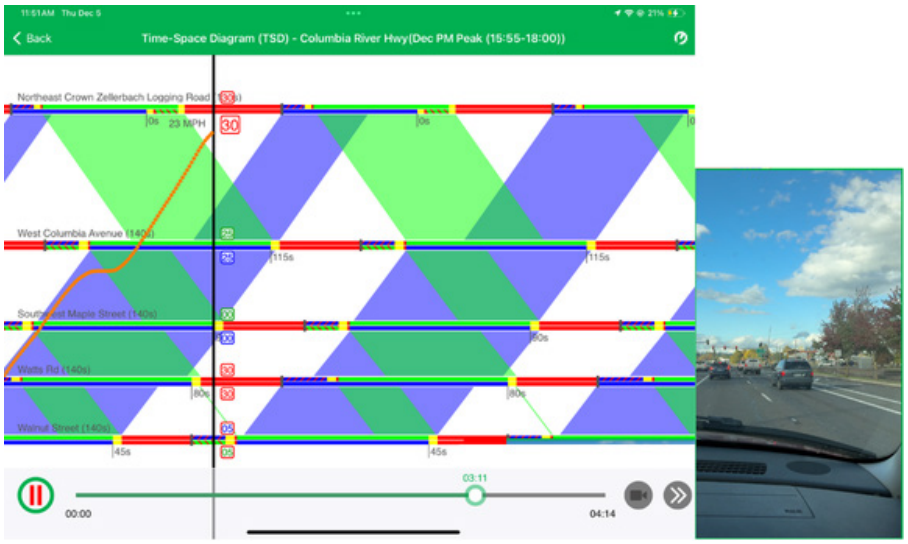

Figure 8. WaySync-M in the Field

3.2 Q-FREE CONTROLLER

Five Q-Free traffic signal controllers were purchased and configured to function as components of the HILS system shown in Figure 9. The Q-Free 2070LDX Controller uses a Linux based operating system running Linux kernel version 3.2 and offers compliance with all latest industry standards including ATC 5201, ATC 6.25, and ATC 5401 (Q-Free, 2024). Additionally, this unit includes built in ethernet ports and hardware/software compliant with latest standards (Q-Free, 2024). Additionally, the ability to configure static IP addresses to the signal controllers allowed for communication between PTV VISSIM and PASS.

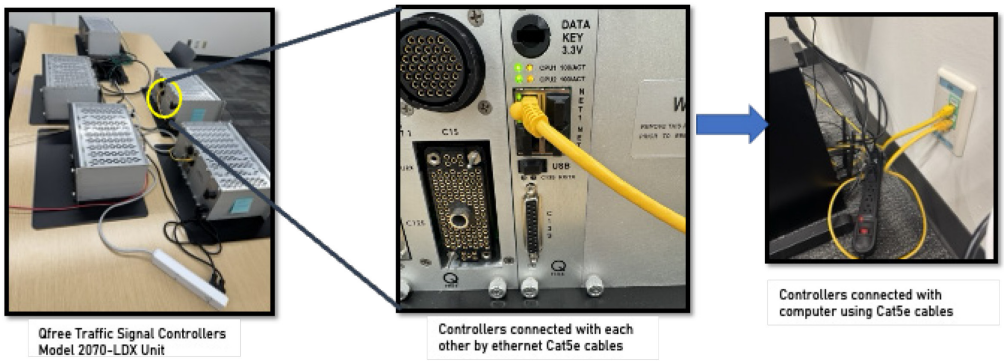

Figure 9. Q-Free Controller Setup

Communication between the signal controllers and the host computer in the HILS was possible via cat5e ethernet cables. This setup enabled two-way communication between controllers and the PTV VISSIM microsimulation model, with PASS acting as a bridge between the two. This connection allowed coordination across all equipment and software, permitting the signal controllers to receive calls from the simulation and relay timing parameters in real-time using. Static IP addresses can be changed or manipulated as needed but must be changed uniformly across all platforms to minimize error and permit communication between equipment.

4.0 METHODOLOGY

4.1 MICROSIMULATION AND HARDWARE INTEGRATION

Ensuring all hardware/cable interfaces are correctly connected was the first step to integrating the traffic signal controllers into the simulation network. The pre-assigned static IP addresses were then used to facilitate communication across all HILS components. A flowchart of the global data flow is described in Figure 10. Key aspects that should be considered from this image include how data is transferred between PTV VISSIM, PASS, and the traffic signal controllers. Notable steps in this process include operating the PTV VISSIM model as usual but transferring service calls through PASS to the signal controllers, the call data is then processed by the signal controllers and the resulting signal display data is relayed back to PASS, which is then able to overwrite the PTV VISSIM controllers while considering hardware integration.

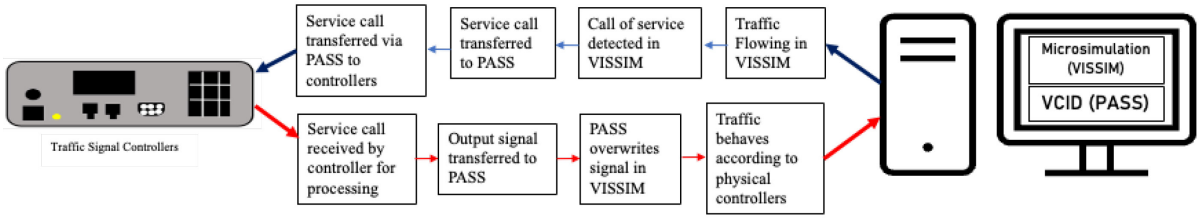

Figure 10. HILS Data Flow

To achieve the dataflow described in Figure 8, setup required all software packages, unique functionalities, and modeling systems to work cohesively. All systems were connected via cat5e ethernet cables and coordinated to work collectively using a text script within the VCID files.

4.2 IDENTIFICATION OF REFERENCE SITE

The base PTV VISSIM model was developed in accordance with Turning Movement Count (TMC) data and pre-existing signal phasing and timing at the reference location along the US 30 highway in Scappoose, Oregon. This corridor features a wide variety of traffic and high vehicular volumes during peak periods, attributes that made it desirable for this pilot study. Site visits at this location revealed that the Winter evening peak-hour, from 4 pm – 6 pm experienced noticeable congestion. An image from the site visit captured on a DJI Mavic 2 Pro drone is shown in Figure 11. Moderate levels of congestion and the presence of heavy vehicles can be detected from visual inspection of the corridor.

Figure 11. Reference Corridor During Evening Peak-Hours

Table 5 describes the minor streets that intersect with US 30 within the confines of the pilot study, as well as whether the intersection is coordinated or isolated, and the vehicular loading volumes at each of these locations. The vehicular volumes were gathered from TMC data obtained through video data analysis to identify the number of vehicles traversing these intersections considering all approaches and turning movements. This shows the total vehicular volumes through the different intersections during the evening peak-hour from 4 pm – 6 pm which was referenced to code the simulation model of the as-built conditions. The four coordinated signals are located at the intersections on the South end of the corridor, while the North end (US 30 and Crown Zellerbach) features an isolated signal in the existing conditions.

Table 5. Intersection Signal Type and Volumetric Loading

Intersection Crossroad	Signal Type	Loading Volumes
Crown Zellerbach	Isolated	5,261
Columbia Ave	Coordinated	5,510
Maple St	Coordinated	5,831
Watts St	Coordinated	5,686
Walnut St	Coordinated	5,532

Drone captured images of the intersections of interest are depicted in Figure 12. From inspecting these aerial images, the largest minor street approaches along the corridor are detected at the Crown Zellerbach intersection. Additionally, one noticeable consideration is that Watts St is a three-legged intersection as compared to the four-leg approaches at the other four locations.

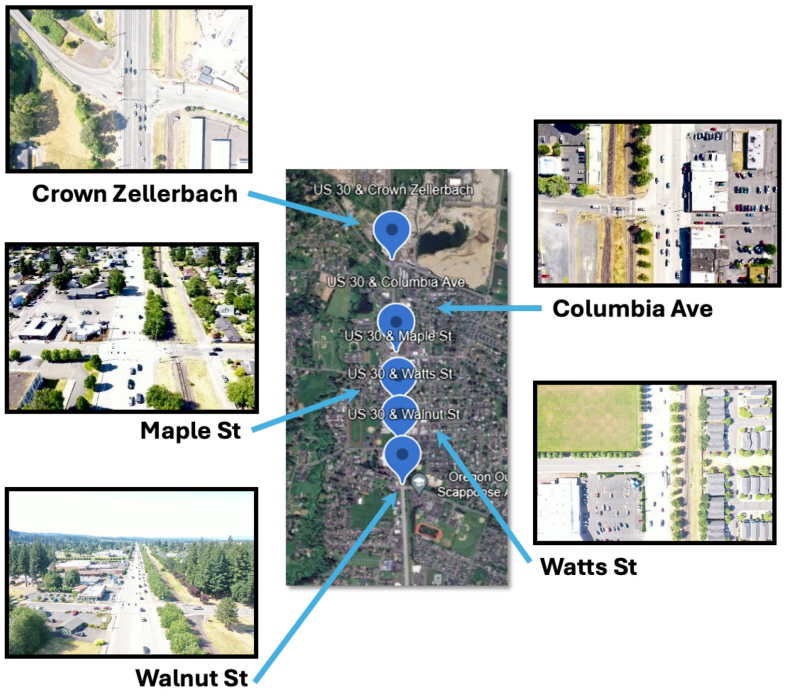

Figure 12. Field Site Corridor Layout and Aerial Images

4.3 MODEL CODING AND CALIBRATION

Coding and calibration of the existing conditions network model in PTV VISSIM started by introducing the collected site characteristics. Information including geometric measurements, TMC data, and signal timings were used to code the existing conditions model. Geometric measurements and TMC data were obtained through site visits and video data collection. Initially, AM and PM weekday peak signal timing plans were also provided by the Oregon Department of Transportation (ODOT). Heavy truck volumes were programmed to be 15% as this aligned with the observed truck density. Figure 13 provides a visual representation of the translation between the field site to the microsimulation at one example intersection. This figure shows the links and connectors that were created and how the field site was referenced in the design process, with an aerial image overlayed in the PTV VISSIM model.

Figure 13. Field to Simulation Comparison for Walnut Street

Calibration procedures for the PTV VISSIM model followed the ODOT Analysis Procedures Manual (APM) protocol for PTV VISSIM simulation (ODOT, 2011). This protocol specifies considerations that should be made during the design process across a wide variety of intersection types, loading volumes, and roadway networks. Although all Sections described in these protocols were addressed, an emphasis was placed on inputs/considerations that were key to the study goals such as: signal controller settings, vehicle routing information, volume and density calibration, and performance evaluation. Following these guidelines, considerations and challenges that were addressed during the calibration procedure include:

- Speed: A spot speed study was not required for signalized intersection corridors due to the difficulty measuring variability (ODOT, 2011).
- Travel Time: Modeled travel time should produce results within ±1 minute for routes with observed travel time less than 7 minutes (ODOT, 2011).
- Queuing: A qualitative comparison of queue lengths is always required while a quantitative comparison is not always required. Qualitative queue length was verified during our site visits.
- Visual Inspection: Simulation modeling outputs were verified via field site visits and review of collected video data.
- Minimum Number of Runs: The model was calibrated using 10 runs with differing seeds as specified by protocols (ODOT, 2011).

A volume calibration procedure was conducted to evaluate Geoffrey E Havers (GEH) values from the output for the peak-hour observation window. The values from the vehicles observed in the field described in Table 2 were used for this procedure alongside the output from the PTV VISSIM simulation. The GEH value is one way to measure the goodness-of-fit of a model (Feldman, 2012). In the case of this study, the GEH value measures how well the simulation models the field data across the peak-hour from 4 pm to 6 pm. The GEH equation is as follows:

Geoffrey E Havers Equation

(4-1)

$$GEH = \sqrt{\frac{2 \times (m-c)^2}{m+c}}$$

m = vehicles in simulation

c = vehicles according to field study

In the case of traffic modeling, a GEH value of less than 5.0 is said to be a "good match" between the modeled and observed volumes (De Villa et. al., 2014). Using this value, 5.0 was determined to be the desirable threshold. All approaches showed GEH values less than 5.0 and

these inputs were replicated in the HILS microsimulation model. GEH values at all approaches disaggregated to 15 minutes intervals are presented in Appendix A.

4.4 EXPERIMENTAL DESIGN

It has been proposed that by manipulating certain elements of the signals at each of the intersections within the corridor, improvements can be achieved. Various aspects of the signalized corridor were identified that were proposed to impact functionality during peak periods. These were subsequently manipulated, and the performance measures were assessed across the various models. Fifteen total models were developed for each of the experimental scenarios, with each model being run three times to collect data. Three trial runs per model was recommended as a good balance of accuracy and efficiency without requiring extensive time for the simulation to complete. This resulted in a total of 45 simulation trials. Each trial ran for 2 full hours, requiring 90 hours of simulation runs. Table 6 describes the various model variables and variable levels that were manipulated and the associated parameter that each variable would impact.

Table 6. Model Variables and Performance Impact

Variable	# of Levels	Levels Description	Impacts
Bi-directional Coordination	4	AM-Peak As-built AM-Peak Fully Optimized PM-Peak As-built PM-Peak Fully Optimized	Corridor functionality
PM-Peak Cycle Length	5	70 seconds 80 seconds 90 seconds 100 seconds 110 seconds	Potential for improved performance
Leading Pedestrian Interval Duration	6	3 seconds 3 seconds Optimized 5 seconds 5 seconds Optimized 7 seconds 7 seconds Optimized	Impact of LPI on intersection performance

The reference location and as-built conditions included five intersections, four of which were coordinated in the existing conditions. Notably, this coordination only applied to one direction of travel in each peak time-period (Southbound in the AM, Northbound in the PM). To understand the impact of using signal optimization to improve the operational performance of the corridor, the fully coordinated variable level featured all five signals in coordination, manipulated offset times to create cohesion across all intersections, and considered coordination in both directions of travel. These models are referred to as the optimized state, where corridor functionality has been optimized to best accommodate all approaches based on site parameters and loading volumes. In addition to bi-directional coordination, models including shorter cycle lengths were designed to understand the impact on performance along the corridor. To identify the threshold

levels, Webster's Formula for Optimal Cycle Length was used and is discussed further detail in Section 4.7.2.

Leading Pedestrian Intervals (LPI) are a type of signal phasing that provides crossing pedestrians with a walk signal before drivers that would present a turning conflict risk for a permitted right turn movement at a given crossing (PBOT, 2024). This phase prevents conflicting vehicle maneuvers entirely, restricting even permissive movements during the duration of the LPI for safety reasons. This allows pedestrians to begin their crossing maneuver before drivers begin to turn and has been proven to reduce collisions by as much as 60% (NACTO, 2013). The impact when including LPI's of three varying durations (3 seconds, 5 seconds, 7 seconds) while considering optimized or non-optimized timing parameters was evaluated, resulting in 6 simulation models. . The optimized conditions in this model consider bi-directional coordination and modified timings across all intersections in the corridor while the non-optimized state represents as built conditions.

4.5 ASSESSMENT OF AS-BUILT CONDITIONS

To assess the precision of the model and provide guidance on key considerations when evaluating future models, results of the existing conditions using the as-built model were extracted. 15-minute intervals were segmented to align with the APM Protocols for VISSIM Simulation procedural process (ODOT, 2011). The performance measures selected as primary interest for the coordinated corridor included: level of service (LOS), average vehicle delay, average maximum queue length, average stop delay, average number of stops, and travel time. A portion of the results have been tabulated for each performance measure within this Section, while all findings can be found in Appendix A.

Average vehicle delay in seconds was used to identify the LOS along each approach and highlight potential areas for improvement. The PTV VISSIM 11 User Manual specifies that, in accordance with guidelines provided in the Highway Capacity Manual (HCM), at signalized intersections, delay times less than 10 seconds reflect LOS A, between 10 to 20 seconds is LOS B, between 20 to 35 seconds is LOS C, 35 to 55 seconds is LOS D, 55 to 80 seconds is LOS E, and greater than 80 seconds is LOS F (PTV, 2018; HCM, 2022). Evaluation of the average vehicle delay output from the HILS system revealed that just under 50% of the approaches in 15-minute intervals had a LOS A. This means that nearly half of the turning movements are functioning very well with minimal delays. These approaches consist of through movements, in the Northbound and Southbound directions. Alternatively, 30% of the approaches along the corridor had an LOS of E or F, indicating that there may be an opportunity to address vehicle delay and congestion at those locations. The largest average vehicle delays observed were located on Eastbound and Westbound approaches. The complete delay results are included in Appendix A.

Average maximum queue length on each approach was also observed. Table 7 describes a portion of this data. Evaluation of all approaches revealed that the upper bound for the average max queue length for through movements at the coordinated intersections occurred on the Columbia NBT movement (533 feet), followed by 318 feet at Walnut NBT movement. At the isolated signalized intersection, the maximum queue length was 773 feet, which occurred during the 5:00 to 5:15 PM interval. The average max queue length for right turning movements had an

upper bound of 606 feet along the Watts EBR movement during the 4:45 to 5:00 PM interval, while the upper bound for left turning movements occurred at the Watts EBL with a queue length of 590 feet.

Table 7. Average Maximum Queue Length (partial results)

Intersection	Approach	Max Average Q length (ft)
Walnut	NBT	318.4
Columbia	NBT	593.1
Crown	NBT	773.3
Watts	EBR	606.7
Maple	EBR	273.9

One noticeable outcome evaluating the maximum queue length results is that, when assessing the right and left turning movements, the largest queue length distance (Watts EBL) was also associated with the maximum average vehicle delay. This agreement supports the modeling results, as a larger delay will generally correlated with larger queue lengths. Detailed average maximum queue length results at each approach disaggregated in intervals of 15 minutes are shown in Appendix A. Evaluation of the average stop delay, and average number of stops revealed that approaches with a left or right turning movement, especially those in the Eastbound or Westbound direction, tended to have higher stop delays and average number of stops. Watts St was found to be associated with the largest stop delay. Detailed number of stops and stop delay on each approach are provided in Appendix A.

Travel time for vehicles between Walnut Blvd and Crown Zellerbach, both Northbound and Southbound, was measured under existing conditions. Measurements obtained from microsimulation using HILS were consistent with field observations under the margins allowed for by ODOT's calibration parameters. Table 8 presents the travel time data for both northbound and southbound movements. Travel time was assessed for 15-minute intervals in alignment with ODOT APM Protocols for VISSIM Simulation. The reported time intervals shown in Table 8 describe the time in seconds elapsed within the microsimulation environment beginning at the start of the PM-peak period. The assessment window begins at 1,800 seconds (i.e., 4:30 pm) as the PTV VISSIM model required 30-minutes of "warmup" time to allow loading volumes to reach a representative state. Therefore, this table shows travel times across a 1-hour observation window starting at 4:30 pm (1,800 seconds elapsed) and ending at 5:30 pm (5,400 seconds elapsed).

Table 8. HILS Travel Time Measurements

Through Direction	Time Interval in Microsimulation (s)	Time (s)
Northbound Through (Walnut to Crown)	1,800 – 2,700	148.6
Northbound Through (Walnut to Crown)	2,700 – 3,600	149.2
Northbound Through (Walnut to Crown)	3,600 – 4,500	147.38
Northbound Through (Walnut to Crown)	4,500 – 5,400	148.9
Southbound Through (Crown to Walnut)	1,800 – 2,700	132.1
Southbound Through (Crown to Walnut)	2,700 – 3,600	134.13
Southbound Through (Crown to Walnut)	3,600 – 4,500	136.7
Southbound Through (Crown to Walnut)	4,500 – 5,400	135.15

4.6 PROBE VEHICLE TRAJECTORY DATA

Upon modeling and calibrating the existing conditions along the US 30 highway, a subsequent site visit was carried out to verify the signal timing plans within the microsimulation in both the Northbound and Southbound direction. This site visit involved traversing the corridor in an outfitted probe vehicle while simultaneously monitoring live vehicle trajectory data using Waysync-M installed on a seventh-generation iPad Pro to provide certainty about the quality of the model. Direct assessments were made during the AM and PM peak hours (6:00 AM to 8:00 AM and 4:00 PM to 6:00 PM). This involved traversing the corridor while recording a live TSD across multiple trials, which was closely monitored to verify that the signal timings displayed in the field matched what was displayed within the microsimulation. It was subsequently confirmed that the microsimulation model was accurately calibrated to the as-built field conditions. The process for recording data while traversing the corridor is shown in Figure 14, where WaySync-M is being used to record and monitor the trajectory throughout the process.

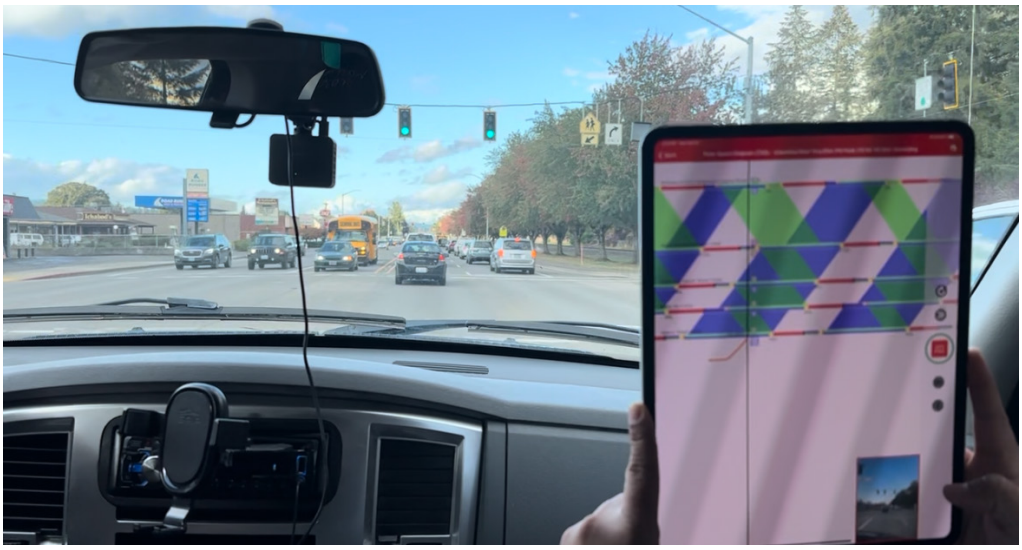

Figure 14. In-Vehicle Perspective of Trajectory Data Collection

The as-built AM-peak timing parameters featured a cycle length of 120 seconds. The unidirectional coordination in signal phasing meant that the Southbound direction of traffic features well designed coordination across multiple signals during this period. This coordination is reflected in the TSD plot displayed in Figure 15, where the solid-green sequences between intersections reflect stable flow in the Southbound direction for those traveling within these boundaries. Alternatively, the Northbound direction is represented as the blue sequences and features comparatively little coordination. The trendline data shows the probe vehicle stops in response to red indications which aligned well with the TSD and field timings, providing certainty about the accuracy of the model.

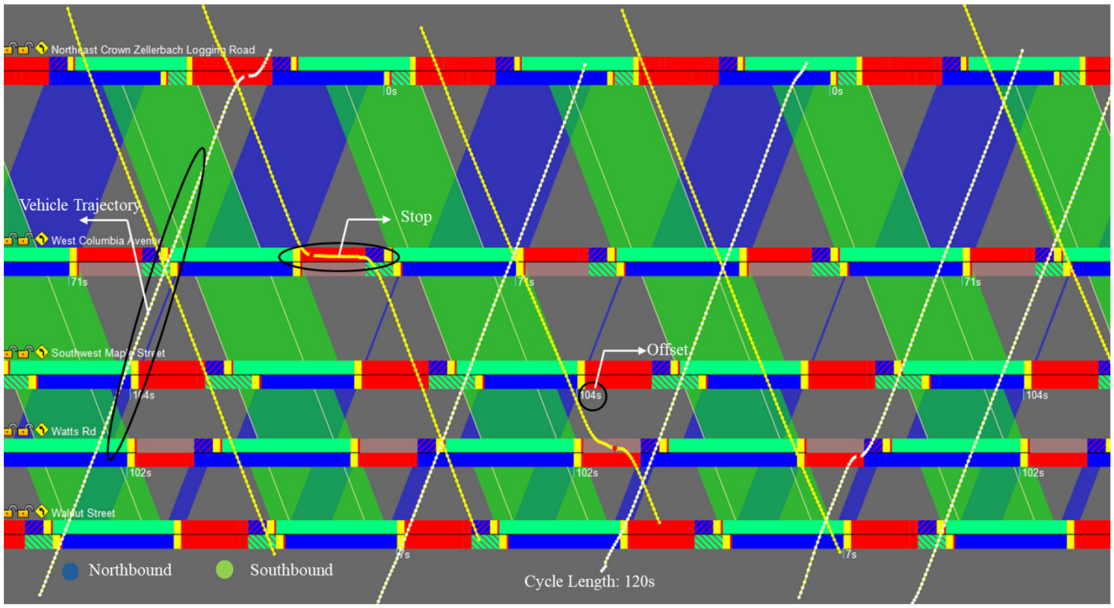

Figure 15. AM-Peak TSD in As-Built Condition

The as-built PM-peak timing parameters featured a cycle length of 140 seconds. This longer cycle length is illustrated by the wider bandwidth of the TSD sequences displayed in Figure 16. Notable observations from the probe vehicle trajectory data in the PM period include the impact of the coordinated signal phasing, where the probe vehicle had less obstructed flow when operating within the boundaries of the coordinated signal plan in the Northbound direction.

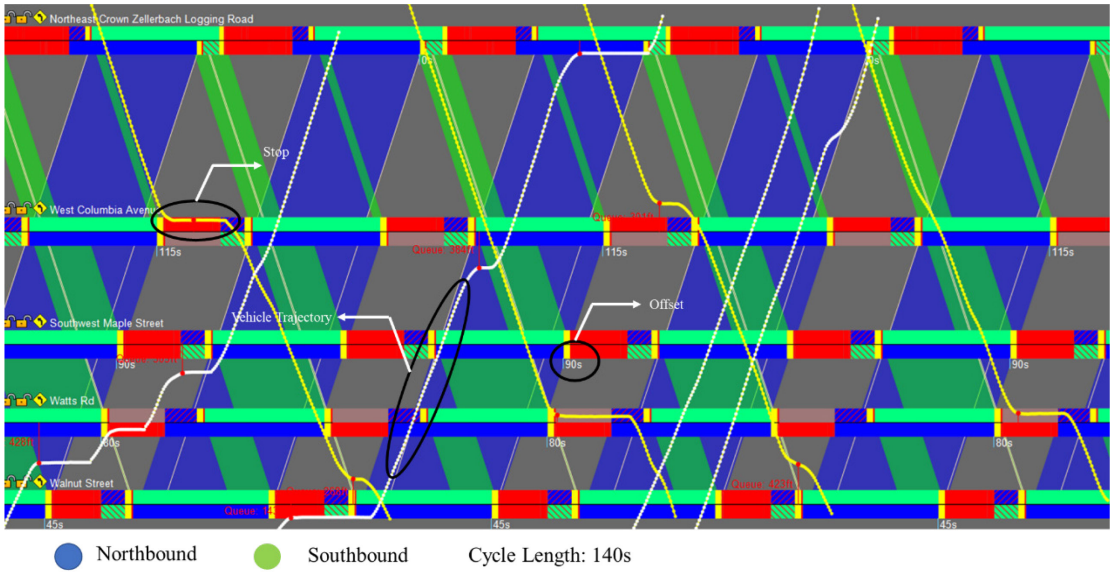

Figure 16. PM-Peak TSD in As-Built Condition

4.7 DESIGN OF VARIOUS MODELS

Subsequent microsimulation models were developed within PTV VISSIM following the successful design and calibration of the existing conditions along the Scappoose corridor. The new models featured manipulation of the signal optimization to align with both directions simultaneously, modifications to the cycle length to test the impact of shorter designs, and the inclusion of leading pedestrian intervals on the overall system. In all microsimulation models, the number of trajectory vehicles for performance assessment was set to 200 vehicles per hour. This value exceeds the minimum required threshold of 100 trajectory vehicles per hour (Wang, 2020).

4.7.1 Bi-Directional Coordination

One method for coordinating the signal phasing involves manipulating the offset time for each intersection in the corridor to accommodate travel time from adjacent intersections (Koonce & Rodegerdts, 2008). Offset refers to the difference in time from a reference point at an upstream intersection to the same point in the cycle a downstream intersection (FHWA, 2022). This time in seconds was manipulated for each of the five intersections of interest to derive coordinated timings along the modeled corridor. The result of the bi-direction coordination plan includes signal phasing that is coordinated in both directions of travel. The 120-second cycle length was optimized for the AM-peak by adjusting the offset time in seconds for each intersection within the corridor. Table 9 compares the as-built conditions to the optimized timings that was found

using the WaySync-D platform, while Table 10 compares the same timing parameters but with a focus on the PM-peak period.

Table 9. AM-Peak Offset for Optimized Cycle

Intersection	Cycle Length (s)	As Built Offset (s)	Optimized Offset (s)
Crown Zellerbach	120	0	57
Columbia Ave	120	71	116
Maple St	120	104	113
Watts Rd	120	102	10
Walnut St	120	7	60

Table 10. PM-Peak Offset for Optimized Cycle

Intersection	Cycle Length (s)	As Built Offset (s)	Optimized Offset (s)
Crown Zellerbach	140	0	71
Columbia Ave	140	115	13
Maple St	140	90	6
Watts Rd	140	80	23
Walnut St	140	45	85

4.7.2 Shorter Cycle Lengths

To understand performance impacts while considering changes to the overall cycle length, the PM-peak period was manipulated. Due to time limitations and the fact that simulations must be run in real-time, only the PM-peak model was selected for evaluation as it was identified as having higher traffic volumes. Therefore, results from this model would be more conservative and representative of the worst-case scenarios. Five cycle lengths were identified for testing, with each cycle length requiring design of a new model to be run. Use of Webster's Formula for Optimal Cycle Length indicated that the minimum acceptable cycle length for this stretch of roadway is 70 seconds based on an hourly Northbound volume of 1,800 vehicles and a flow ratio of 0.5. Seventy seconds was subsequently used as the bottom threshold when assessing the impact of this variable level. Additional assessments were carried out at 10 second increments when interpolating from 70 seconds to 120 seconds to understand how the performance measures change in response to these adjustments. Webster's Formula for Optimal Cycle Length includes the following equation:

Webster's Formula for Optimal Cycle Length

(4-2)

$$C = \frac{1.5L + 5}{1 - Y}$$

Each cycle length model required the intersections to be optimized to meet the new timing parameters. This process involved manipulation of the offset time to achieve an optimized corridor under the new timing design. The cycle length and corresponding offset time for each intersection is shown in Table 11.

Table 11. Offset Time for Shorter Cycle Lengths

Intersection	Cycle Length (s)	Offset (s)
Crown Zellerbach	70	66
Crown Zellerbach	80	77
Crown Zellerbach	90	35
Crown Zellerbach	100	55
Crown Zellerbach	110	64
Columbia Ave	70	39
Columbia Ave	80	45
Columbia Ave	90	0
Columbia Ave	100	15
Columbia Ave	110	12
Maple St	70	3
Maple St	80	1
Maple St	90	83
Maple St	100	24
Maple St	110	21
Watts Rd	70	8
Watts Rd	80	14
Watts Rd	90	36
Watts Rd	100	22
Watts Rd	110	20
Walnut St	70	40
Walnut St	80	46
Walnut St	90	53
Walnut St	100	59
Walnut St	110	66

4.7.3 Leading Pedestrian Interval

Models considering the impact of LPI's were created and tested. LPI's were designed solely at the intersection of US 30 and Crown Zellerbach and the impacts on vehicle performance at this intersection was assessed. Software packages including Viswalk, which is one method for incorporating LPIs into the PTV VISSIM model, was found to be incompatible with PASS. Additionally, the WaySync-D suite was unable able to accommodate LPIs at the time of this study (This can be resolved, but would require significantly more programming well beyond the scope of what could be accomplished in this project). To address these limitations, signal calls were placed using the Maxtime interface for specific signal phases. The "Advanced Walk" function within Maxtime was modified accordingly for two pedestrian crossing locations

corresponding to phases 4 and 8. Figure 17 shows the pedestrian crossings that were considered in the models, with the Eastbound crossing being associated with signal phases 4 and 8.

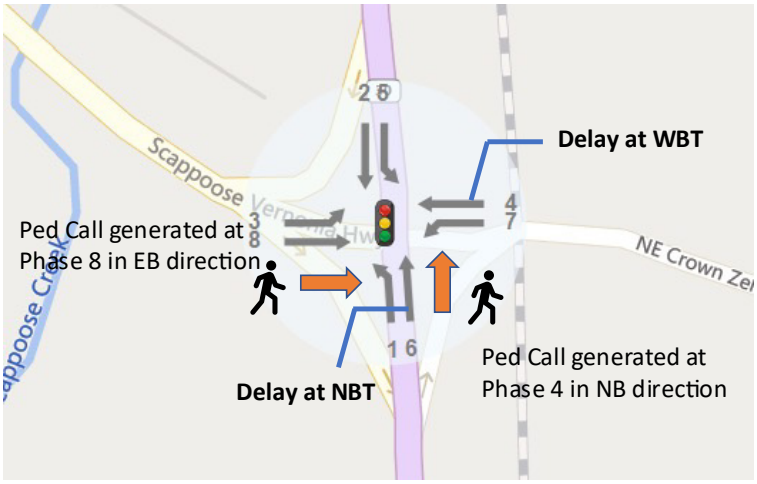

Figure 17. LPI Implementation for NB and WB

Three different levels of LPI timings were tested and included 3, 5, and 7 second advances for crossing maneuvers. Figure 18 shows a screen capture of the MAXTIME UI, illustrating the signal phase status at the Crown Zellerbach & Lodging Rd intersection. From this image, one can observe that signal phases 4 and 8 are currently displaying a "walk" signal, as the Leading Pedestrian Interval (LPI) is active, while all other phases are showing a red signal. Additionally, calls have been placed for queued traffic along the other phases. This information was compared in real time with simulation model to ensure the controller and simulation are well synchronized.

Phase	1	2	3	4	5	6	7	8
Reds	●	●	●	●	●	●	●	●
Yellows								
Greens								
Veh Calls	🚗	🚗	🚗	🚗	🚗	🚗	🚗	🚗
☑ Min Calls	☐	☐	☐	☐	☐	✓	☐	☐
☐ Max Calls	☐	☐	☐	☐	☐	☐	☐	☐
Ped Calls		🚶		🚶		🚶		🚶
☑ Ped Call	☐	🚶	☐	🚶	☐	🚶	☐	🚶
Ped 2 Calls								
Dont Walks		✋				✋		
Ped Clears								
Walks				🚶				🚶

Figure 18. Maxtime Call Placed for LPI Function

5.0 RESULTS

5.1 BI-DIRECTIONAL OPTIMIZATION IN WAYSYNC-D

As-built conditions were compared with the models featuring bi-directional coordination signal timings along the corridor for the AM- and PM-peak periods. The model featuring optimized conditions used WaySync-D to design and test changes made to offset values to achieve cohesion across all five intersections while also considering bi-directional coordination. Vehicle trajectories and corridor performance was assessed with a flow of 200 vehicles per hour. Performance measures included average vehicle delay, stop delay, and number of stops.

5.1.1 AM-Peak Bi-Directional Coordination

Trajectory data for vehicle movements during the AM-peak period is shown in Figure 19. The variations in these two TSD's show how the bi-directional optimization is visually portrayed, with a lack of connectivity in the Northbound direction (blue bandwidths) during the northbound only coordination model in Figure 19. Meanwhile, these same bands are connected in sequence in Figure 19 which shows the final signal timing for bi-directional coordination. WaySync-D also provides callouts when a queue length forms between intersections and is visually portrayed on the TSD using a horizontal line despite being within the zone of a green signal display at the subsequent intersection. The length of the queue directly correlates to the length of the horizontal line, but the degree of differences in the two models is difficult to discern exclusively through visual inspection. To further understand the results, direct measurements were output from each model and compared to quantify the differences. Results were extracted in 15-minute intervals as specified as the recommended form of assessment in a microsimulation setting (ODOT, 2011).

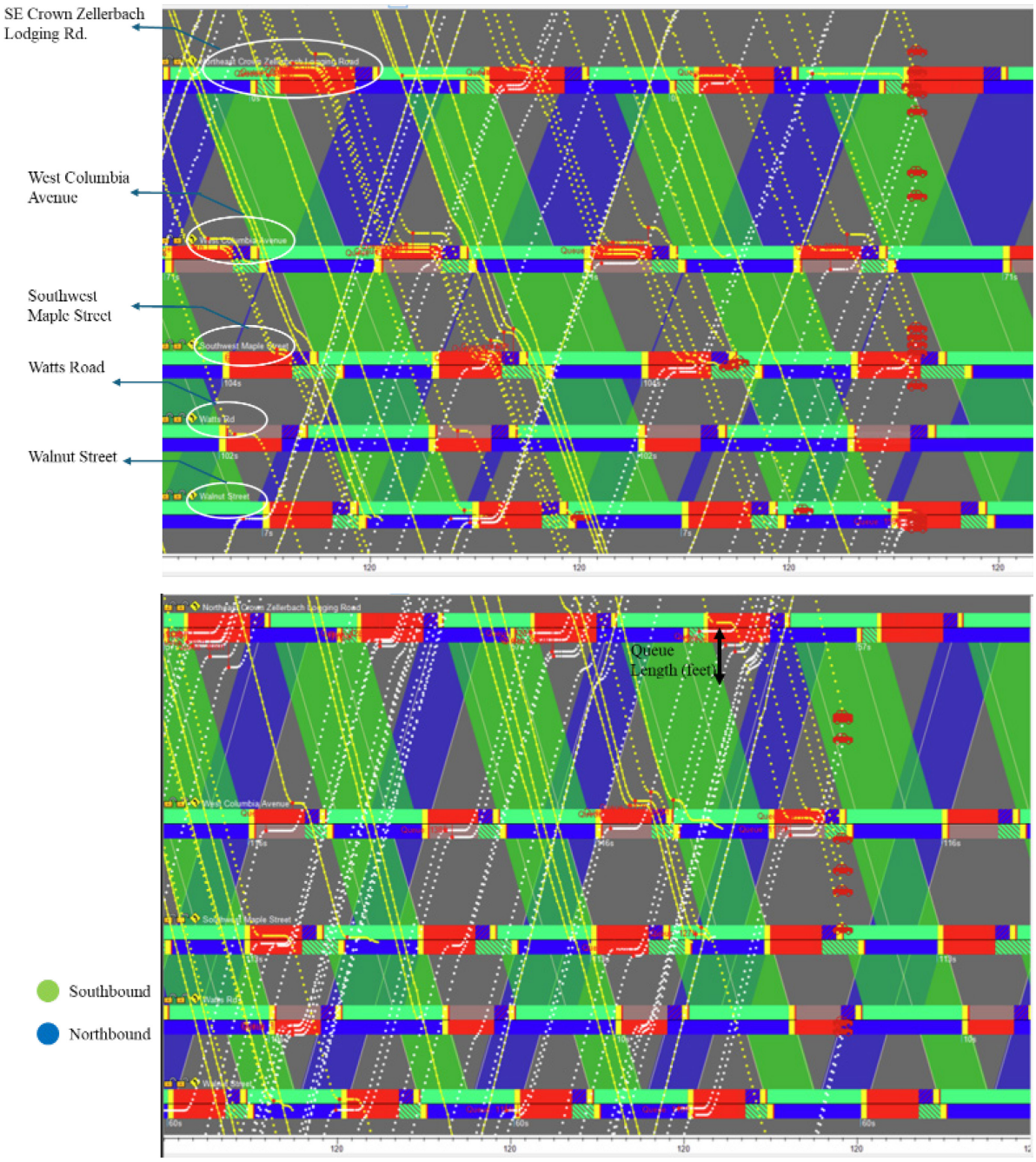

Figure 19. NB (top) and Bi-Directional (bottom) Coordination TSD for AM-Peak

As discerned from the review of prior literature, the most common performance measure for understanding corridor functionality is vehicle delay. Figure 20 describes the average vehicle delay along the mainline (US 30) for through-moving vehicles in the Northbound (left) and Southbound (right) directions of travel for the two model scenarios. This figure highlights the decrease in vehicle delay in the Southbound direction at the Maple St intersection, which reduced from 5.6 seconds to 1.0 seconds. Additionally, Colombia Ave and Watts St also display a decrease in travel time. Slight variations in vehicle delay are observed in the Northbound

direction, with the most prominent increase upon running the bi-directional coordination model being at the Crown Zellerbach intersection. Due to this increase of approximately 8.0 seconds, the LOS at this intersection for Northbound through movements went from a LOS A to a LOS B in the optimized conditions.

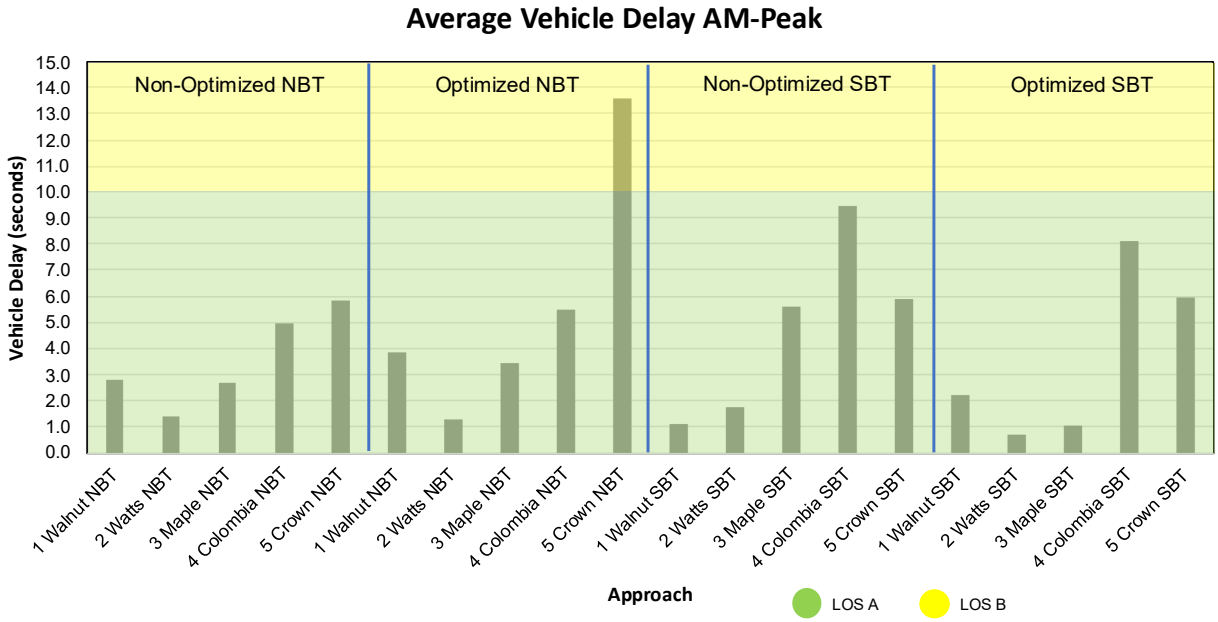

Figure 20. NBT and SBT Vehicle Delay During AM-Peak

It may appear counterintuitive that some intersections experienced larger delays in the optimized models. This is likely a result of the timing plan also considering vehicles along the minor road traveling in the Eastbound and Westbound directions. It is proposed that this contributed to the 8.0 second increase in delay experienced by the Northbound traffic at the Crown Zellerbach intersection. This delay increase is minimal in comparison to the reduction observed in the Eastbound and Westbound directions at Crown Zellerbach, where through movements had decreased delays of up to 22 seconds and 50 seconds, respectively. This helped achieve an improved LOS, where the Eastbound direction improved from a LOS E to a LOS D while the Westbound direction changed from a LOS F to a LOS D. This result indicates that to fully understand and assess the impact of the optimized plan, all movements must be considered. Average vehicle delay for through-moving vehicles at each intersection across all approaches and their associated LOS values are tabulated in Table 12. LOS designations followed thresholds defined in the Highway Capacity Manual for delay at signalized intersections (HCM, 2022).

Evaluation of the average number of stops revealed consistent output when considering the through moving traffic. Southbound traffic experienced an improvement at the Maple St intersection while tradeoffs can be observed at the Crown Zellerbach intersection. Figure 17 shows the average number of stops at the Crown Zellerbach intersection for through movements in various directions of travel.

Table 12. AM-Peak Average Vehicle Delay and LOS Changes

Direction of Travel	Model	Walnut	Watts	Maple	Colombia	Crown
Eastbound	As-built	64.0	N/A	71.7	N/A	61.9
	Optimized	67.9	N/A	74.9	N/A	55.3
	LOS change	--	--	--	--	**E → D**
Westbound	As-built	98.3	N/A	9.2	47.2	73.3
	Optimized	104	N/A	9.2	28.4	46.3
	LOS change	--	--	--	**D → C**	**F → D**
Northbound	As-built	2.8	1.4	2.7	4.9	5.9
	Optimized	3.9	1.3	3.4	5.5	13.6
	LOS change	--	--	--	-	**A → B**
Southbound	As-built	1.1	1.8	5.6	9.5	5.9
	Optimized	2.2	0.7	1.0	8.1	5.9
	LOS change	--	--	--	--	--

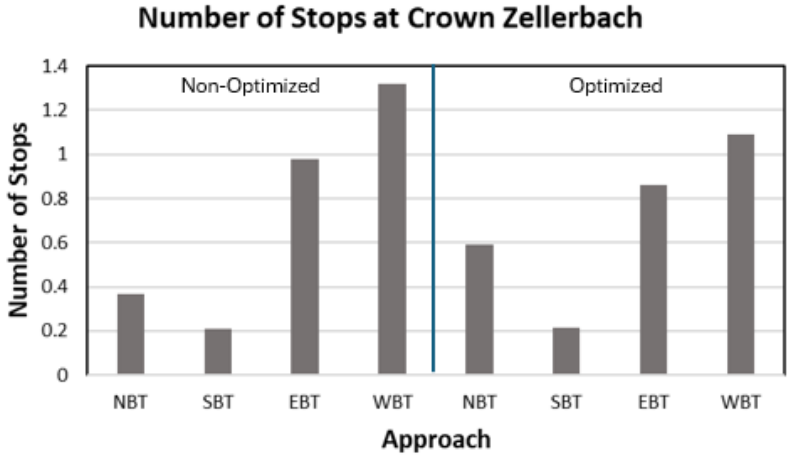

Figure 21. Number of Stops at Crown Zellerbach for All Approaches

Although through-moving vehicles were a primary focus, turning movements were also evaluated and compared across models. One notable outcome is the improved reduction in vehicle stop delay when considering those queued to turn left. In the non-optimized models, vehicle stop delay reached peak values of 130.0 seconds for Southbound traffic at the Crown Zellerbach intersection. In the case of the optimized models, stop delay reduced by 40.0 seconds for the same location and evaluation period. Similarly, the stop delays for vehicles in the Northbound direction completing a left-turn maneuver had an average reduction of 9.0 seconds. The plots for stop delay at each intersection can be found in Appendix B.

5.1.2 PM-Peak Bi-Directional Coordination

Adjustments to the PM-peak period bi-directional coordination across the entire corridor with the improved functionality of Southbound movements. This is represented visually in Figure 22 through the connectivity of vertical bands. In the existing conditions, the Northbound direction is coordinated at all intersections except for the Crown Zellerbach location. Meanwhile, the lack of connectivity in the Southbound direction indicates that none of the signalizations were coordinated. These issues are resolved upon inspection of the optimized model, which shows how modifications to the offset timing parameters impacts flow throughout the corridor. Trajectory data for the 200 vehicles per hour reveal that Northbound vehicles beginning their movements within the boundaries of the coordination, like those in the center of the TSD, were able to travel consistently through all intersections with a reduced likelihood of encountering a queue. In the Southbound direction, more consistent results were observed in the optimized model and queue length impacts were visually less pronounced.

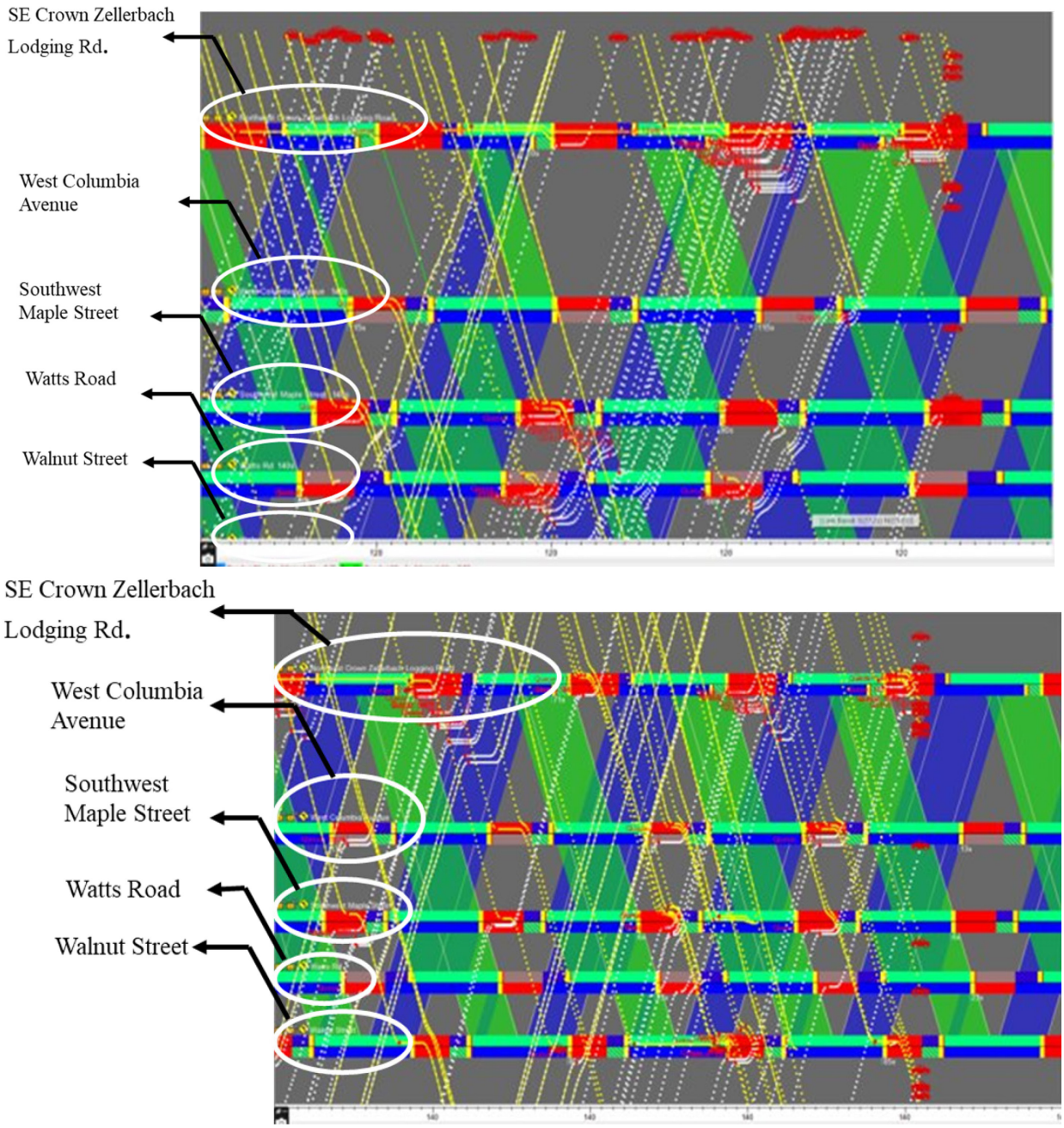

Figure 22. SB (top) and Bi-Directional (bottom) Coordination TSD for PM-Peak

Evaluation of the performance measures indicated that one of the most notable changes with the PM-peak period assessment is how the optimized model improved the accessibility for vehicles turning onto the mainline. Specifically, how coordinating and optimizing timings in the Southbound direction allowed for increased accessibility for those on the minor streets. A prime example of this is the Eastbound traffic at Watts Rd. Right-turning vehicles tended to have a vehicle delay approaching 500 seconds in the as-built conditions, representing a LOS F. These vehicles were believed to experience more difficulty turning right onto the Southbound approach in this model due to the lack of optimization during the PM-peak. By implementing the

optimized timing plan, right-turning traffic from Watts Rd decreased in delay by 39.8% on average while the queue lengths decreased by 194 ft. Additionally, left-turning vehicles (turning into the Northbound flow) experienced an average delay reduction of 211 seconds during the last 15-minute observation window. Figure 23 provides visualizations of these improvements along the Eastbound approach considering traffic turning onto the mainline from Watts Rd.

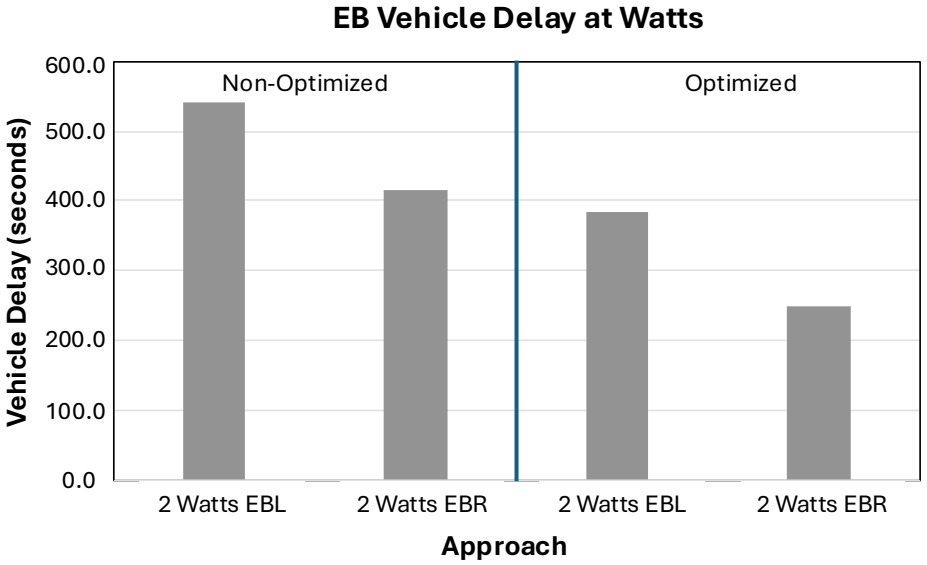

Figure 23. EBL and EBR Vehicle Delay

The vehicle delay experienced along the Northbound and Southbound directions of travel is described in Figure 24. From this data for through-moving vehicles, a delay increase can be observed similar to that of the AM-peak assessment, but the degree of increase is minimal in comparison to the improvements along the minor approaches. Recall that a delay of 10 seconds or less classifies as a LOS A (HCM, 2022). Across all intersections, Northbound and Southbound traffic still achieved a LOS A while also generating improvements along the minor street when the optimized model was considered. The largest delay was found to be 9.75 seconds on average and occurred at the Crown Zellerbach intersection for Northbound traffic.

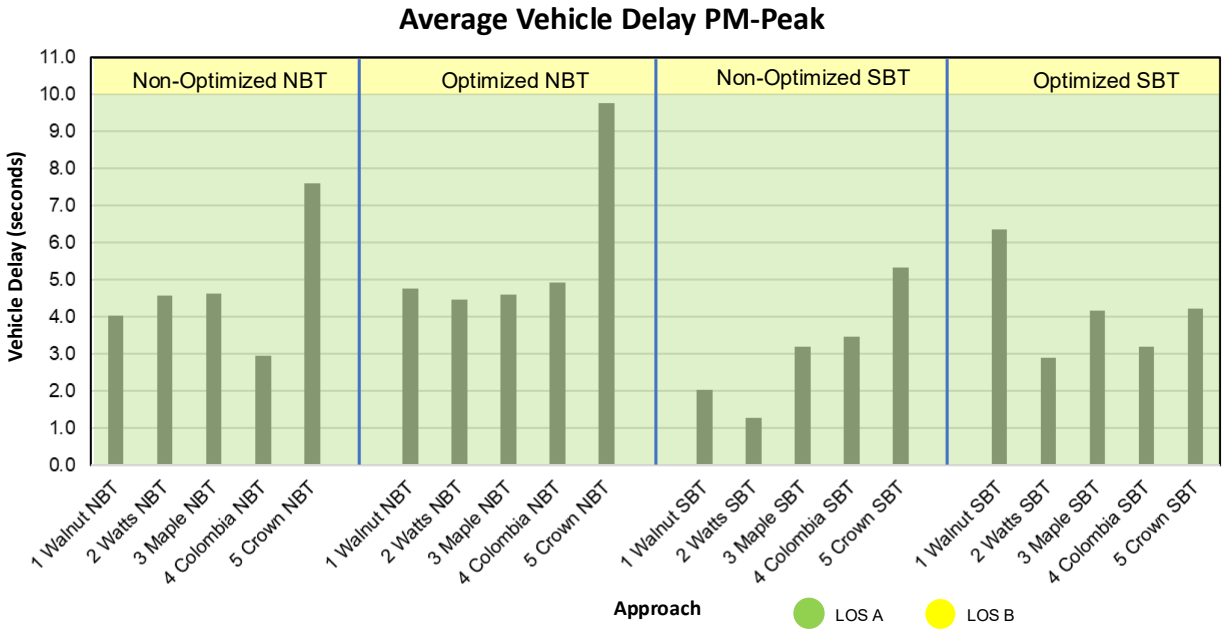

Figure 24. NBT and SBT Vehicle Delay During PM-Peak

Table 13 documents all movements during the PM-Peak that experienced a change in LOS when comparing the two models. This data shows that there was an equal number of movements that experienced an improved LOS as compared to those that experienced a reduced LOS. That being said, majority of the movements that experienced a reduced LOS were minor street approaches at the Crown Zellerbach intersection, which may be due to a lack of coordination and thus longer green displays for the minor street in the as-built configuration.

Table 13. PM-Peak Average Vehicle Delay and LOS Changes for All Movements

Improvement / Reduction	Approach	Turning Maneuver	Intersection	As-built	Optimized	LOS Change
Improved LOS	Eastbound	Right	Walnut St	11.0	9.3	B → A
Improved LOS	Westbound	Left Right	Maple St Maple St	82.6 20.1	70.9 13.0	F → E B → A
Improved LOS	Northbound	Left	Watts Rd Colombia Ave	108.2 10.8	79.7 7.6	F → E B → A
Improved LOS	Southbound	Left Left	Maple St Colombia Ave	23.8 20.7	14.2 16.2	C → B C → B
Reduced LOS	Eastbound	Left	Crown	46.3	61.7	D → E
Reduced LOS	Eastbound	Right	Maple St	33.4	103.3	C → F
Reduced LOS	Westbound	Left	Crown	48.0	62.2	D → E
Reduced LOS	Westbound	Right	Crown	43.8	71.1	D → E
Reduced LOS	Westbound	Through	Crown	55.5	104.8	E → F

5.2 SHORTER CYCLE LENGTHS

Models with a variety of cycle lengths were assessed. Five separate configurations were tested in the microsimulation environment during the PM-peak which included cycle lengths of: 70-, 80-, 90-, 100-, and 110 seconds. All results are documented in Appendix B, with the key findings and notable observed differences discussed throughout this Section. Stop delay and vehicle delay were isolated as key performance measures for the various directions of travel and turning maneuvers at each intersection.

From inspection of through movements, an inflection was observed at the midpoint for models using 90 second cycle lengths when evaluating the stop delay results. Evaluation of the Southbound through movements display this observation most distinctly. Figure 25 shows how Colombia Ave was associated with 3.1 second and 4.5 second stop delays in the longer cycle length models but decreased to 2.3 seconds or less when the cycle length was reduced to 90 seconds or lower. This threshold was kept in-mind while assessing the performance measures at adjacent approaches to understand the point at which introduction of shorter cycle lengths produces considerable improvements and less than that produces diminishing returns.

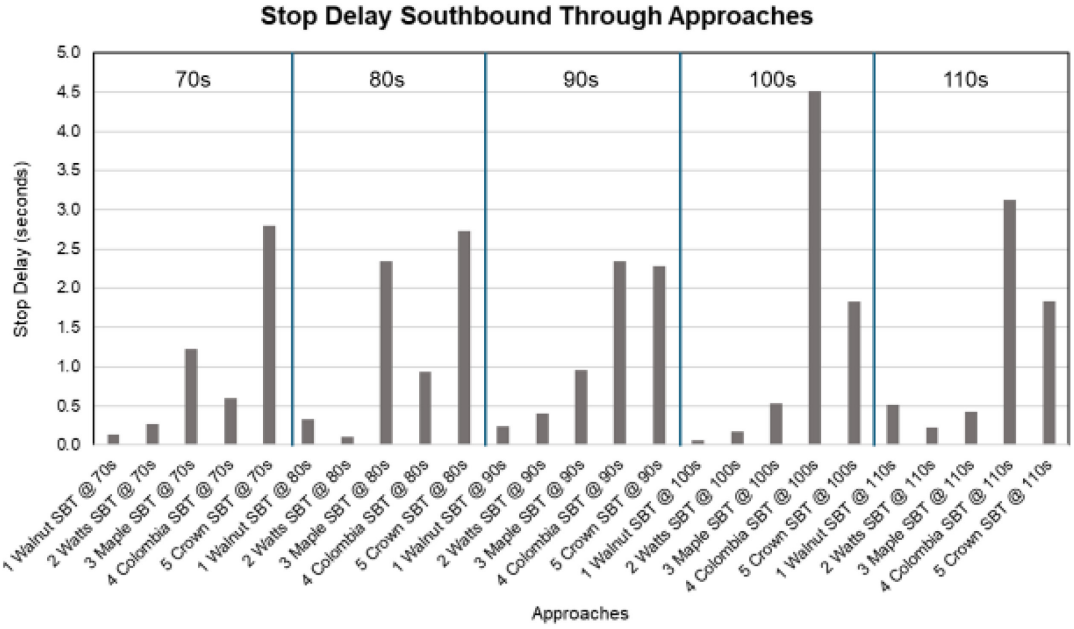

Figure 25. SBT Stop Delay at Various Cycle Lengths

Vehicle delay for through movements in the Northbound direction found a similar result, where transition to a LOS B was found upon modeling cycle lengths of 80 seconds or less at Colombia Northbound through approach. On the other hand, increasing the cycle length beyond 80 seconds led to improvement in LOS at Colombia Northbound through approach. Figure 26 displays vehicle delays at all intersections for the Northbound direction through movements, with a key finding being that a LOS reduction was observed when evaluating the cycle length of 70 and 80 seconds.

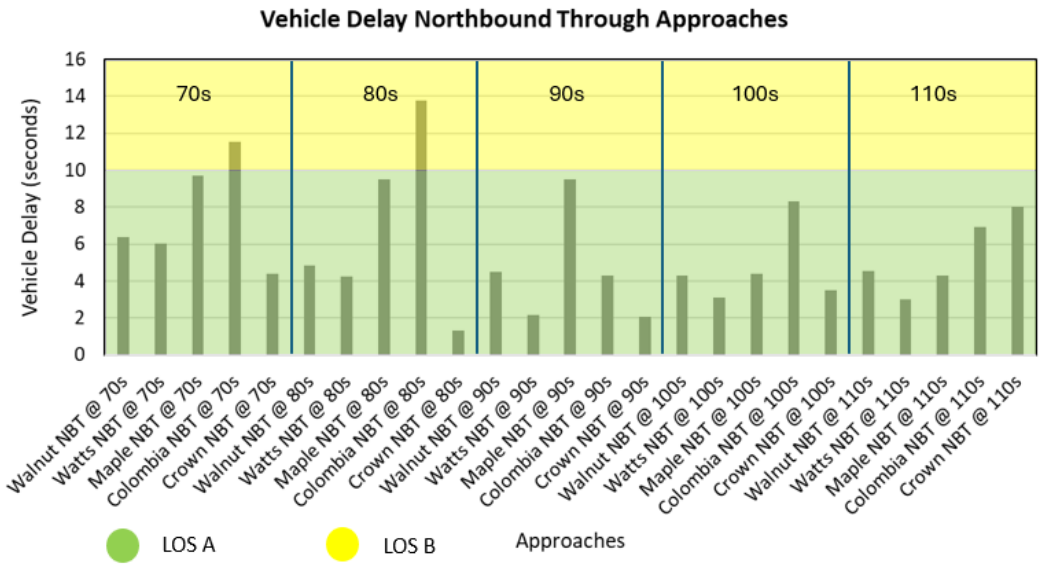

Figure 26. NBT Vehicle Delay at Various Cycle Lengths

Similar to the findings discussed in the optimized PM-peak model, noticeable changes in vehicle delay were observed for Eastbound turning movements at the Watts intersection when evaluating shorter cycle lengths. Meanwhile, the change in performance when comparing the 90 second cycle length to the adjacent models' mimics what was discerned for Northbound and Southbound through movements. Figure 27 describes vehicle delay results for left and right turning vehicles on the Eastbound approach. For both turning maneuvers, the delay was much lower when evaluating the model with 70 second cycle lengths. That being said, 90 second cycle lengths were found to be where improvements became most prominent as delays reduced by over 50% from the longer length models.

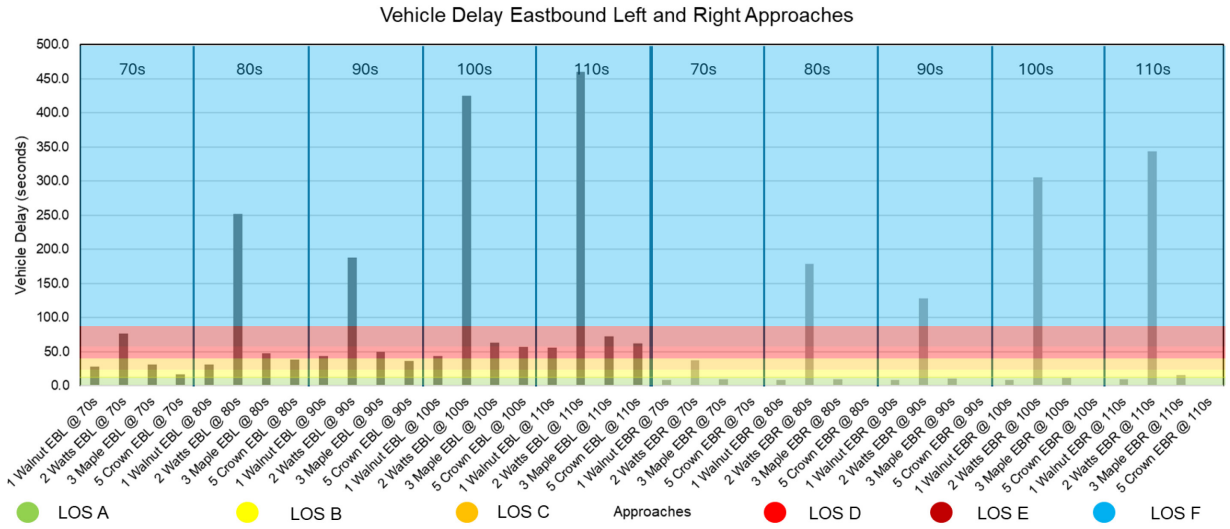

Figure 27. EBL and EBR Vehicle Delay at Various Cycle Lengths

The findings of the Northbound and Southbound through movements paired with the delay for Eastbound turning movements provide evidence that the 90 second model is where improvements become noticeable. Meanwhile, reducing to 80 seconds produced increased delay results for Eastbound approaches. These findings provide supporting evidence that there may be an inflection at the model running cycle lengths of 90 seconds where a further reduction in cycle lengths may not produce noticeable returns in delay or stop-delay reductions.

5.3 LEADING PEDESTRIAN INTERVALS (LPI)

Performance at the Crown Zellerbach intersection for Northbound and Westbound through movements were assessed when considering the inclusion of LPIs of differing lengths. The LPI functioned to give crossing pedestrians a head start before vehicle movements were permitted. This design meant that either 3-, 5-, or 7- seconds prior to the vehicular green were allocated to the crossing phase. Evaluation of the Northbound direction of travel revealed a direct relationship between vehicle delay and the length of the LPI when considering models that were not optimized. Meanwhile, the optimized models revealed promising results in terms of vehicle delay regardless of the length of the LPI, with Northbound traffic experiencing approximately 23 seconds of delay on average in each model. This indicates that, even in scenarios where pedestrians were allocated with more time to cross the intersection (i.e., 5 second or 7 second LPI), using optimized signal timings can lessen the impact of this additional LPI duration. Figure 28 shows these results for the Northbound vehicle delay.

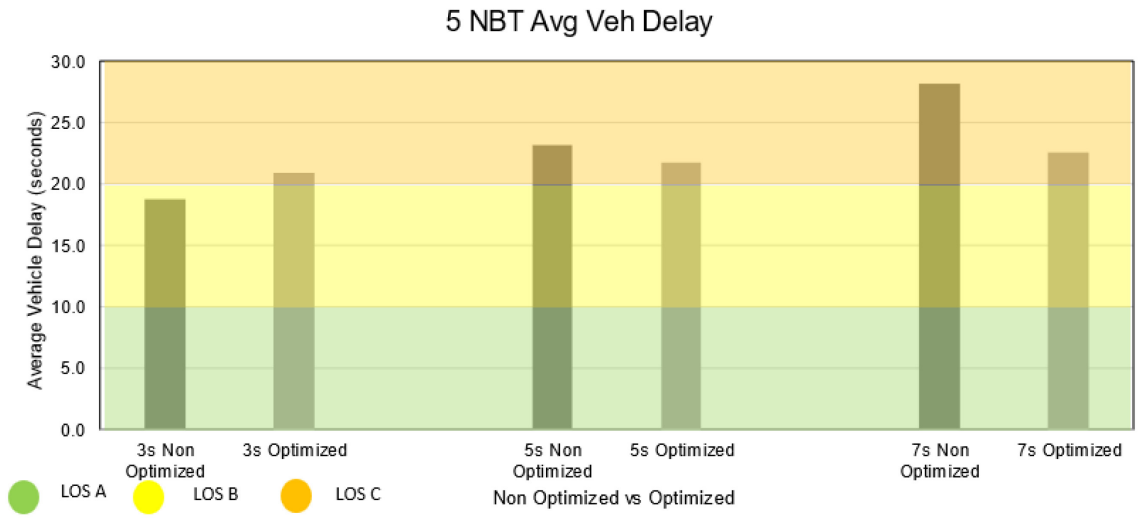

Figure 28. NBT Vehicle Delay at Crown Zellerbach

A similar trend was observed when investigating stop delay for the Northbound vehicles, where a consistent increase was prevalent when considering models that were not optimized. Figure 29 shows these results for each model. The model designed with a 7 second LPI displayed the highest stop delay of 22.5 seconds in non-optimized conditions and 18 seconds when optimized. Despite this finding, comparison with the other models showed that the optimized model retained only a slight increase in stop delay which was found to be approximately 2 seconds longer than the prior models. This indicates that longer LPIs become less impactful when the corridor is

optimized, while shorter LPI lengths may be more suitable at locations that do not feature any optimization.

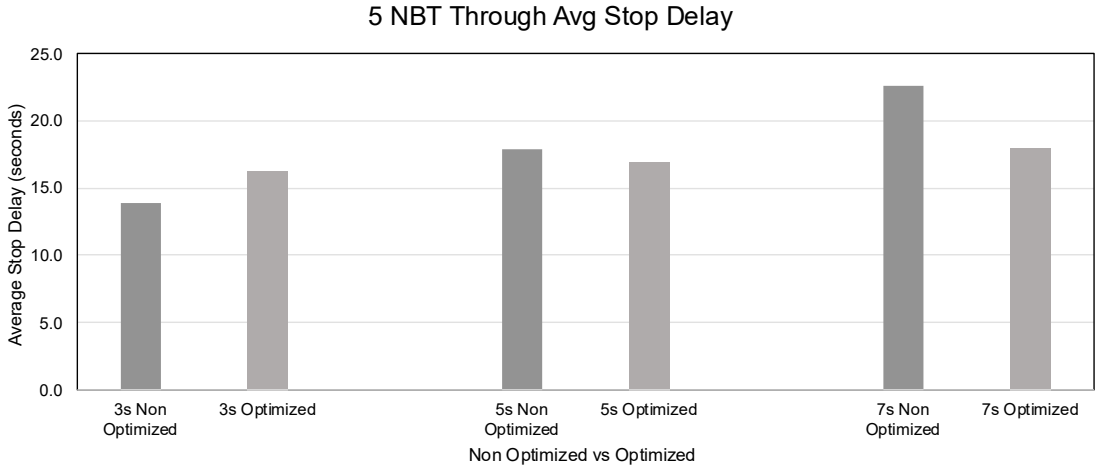

Figure 29. NBT Stop Delay at Crown Zellerbach

The same LPI durations were applied to the Westbound direction of travel and similar performance was assessed. The results of the average vehicle delay are displayed in Figure 30. Contrary to the findings of the Northbound traffic, there was an inverse relationship for vehicle delay when considering an increase in the LPI length across the non-optimized models. Meanwhile, more inconsistent fluctuations in delay were observed when evaluating the optimized conditions. From Figure 30, it can be observed that average vehicle delay was around 65 seconds when considering an LPI of 3 seconds, then increased to 70 seconds when the LPI was increased to 5 seconds, and subsequently dropped to 64.5 seconds when the LPI reached 7 seconds in length; All of which were higher than the vehicle delay experienced in the non-optimized conditions, which was approximately 55 seconds on average. This indicates that certain directions of travel benefit more from the optimized conditions when LPIs are implemented. A similar observation was found when evaluating stop delay, where the optimized conditions displayed the largest average stop delay for Westbound traffic.

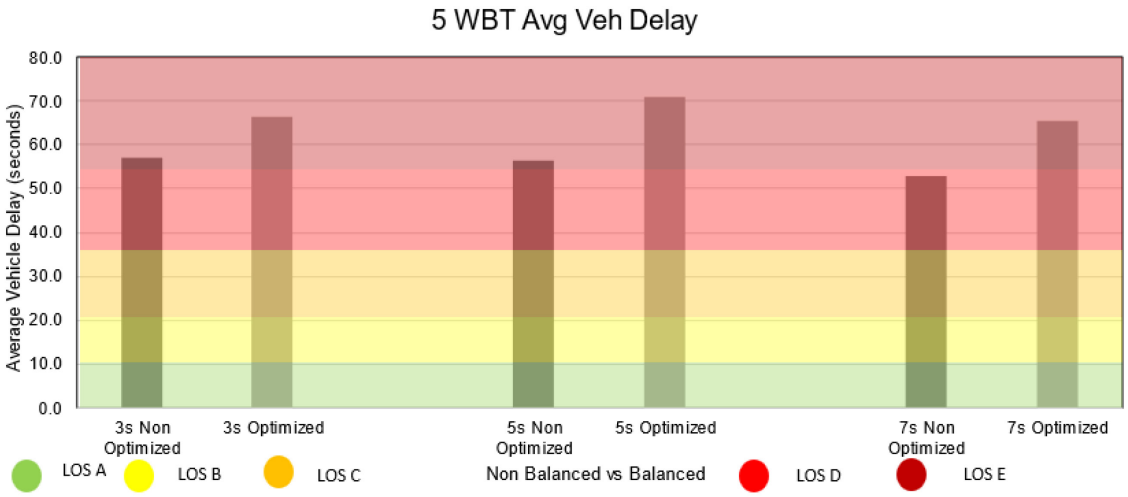

Figure 30. WBT Vehicle Delay at Crown Zellerbach

An interesting finding occurred with the number of stops experienced by vehicles in the Westbound direction of travel. Despite the consistent findings for vehicle delay and stop delay on this approach, the average number of stops was found to be largest in the optimized conditions when considering an LPI of 7 seconds. Although the scale of this chart is smaller than that of the prior, Figure 31 shows that the number of stops was relatively unchanged across all models except for the optimized conditions featuring an LPI of 7 seconds. In this condition, the average number of stops increased by about 30% in comparison to all other models (1.3 stops compared to 1.0 stops on average).

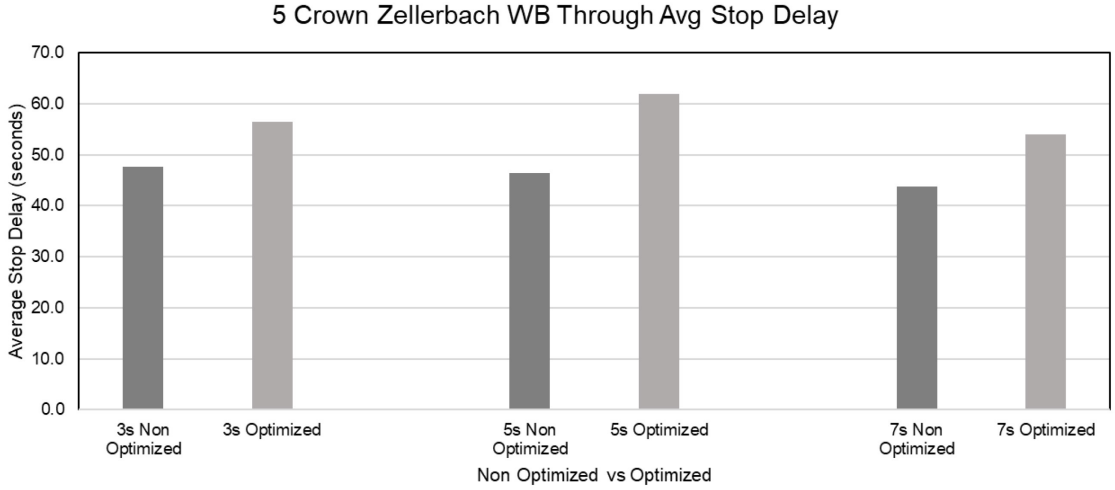

Figure 31. WBT Number of Stops at Crown Zellerbach

The results of the models while considering the influence of an LPI of varying lengths showed that the length of the LPI as well as the optimization of the overall corridor must be considered. For vehicles traveling on the mainline (Northbound), a longer LPI length can be implemented to

give adequate time for the crossing maneuver without drastically increasing the vehicle delay so long as the signalization along the corridor is optimized. In conditions where optimization is not possible, a shorter LPI may be preferred so that delay is not largely impacted by this additional timing unit. Meanwhile, vehicles traveling on the minor approach (Westbound) are impacted more by the optimization as opposed to the LPI length. Findings related to vehicle delay were consistent regardless of the length of the LPI for the Westbound crossing and displayed approximately 55 seconds of delay for all cases. Meanwhile, the optimized models showed increased delay and number of stops when LPIs were implemented. This finding indicates that incorporating LPIs into the overall system has situational considerations that differ based on the approach and existing signal phasing. In the case of this corridor analysis at the Crown Zellerbach intersection, LPI implementation may be most feasible in the Northbound direction when the entire corridor is optimized but there is less justification for its presence in the Westbound direction unless a clear need is present for safety concerns of pedestrians crossing this leg of the intersection.

6.0 CONCLUSIONS

6.1 KEY FINDINGS

This study evaluated the impacts of bi-directional optimization, shorter cycle lengths, and LPI implementation along a 0.93-mile corridor with five signalized intersections. Key findings indicate the potential to cohesively sync software packages and physical signal controllers to evaluate signalized corridors and understand how performance can be improved. This study successfully implemented a HILS with five physical controllers to understand performance impacts under a variety of microsimulation configurations.

Results from the bi-directional optimized models revealed that modifications to the offset values between successive intersections coordinates signals to allow vehicles promotes more consistent flow across the arterial roadway. This resulted in increased performance across the length of the five-signal corridor but close inspection of turning maneuvers was required to recognize all improvements that were created. Although vehicle delay increased at the Crown Zellerbach intersection for the Northbound traffic in the AM- and PM-peak, the increase relative to the decrease in delay for adjacent approaches was reasonable. Eastbound and Westbound throughput delay was found to decrease by up to 19 seconds, and resulted in a LOS decrease at the Crown Zellerbach intersection. This is due to the optimized conditions accommodating all approaches, not solely those traveling along the mainline which was prominent when assessing Eastbound traffic turning onto the mainline during the PM-peak. In these scenarios, left and right turning vehicles had improved accessibility and experienced delay reductions up to 211 seconds when the bi-directional model was designed and optimized. This finding was consistent across other performance measures assessed.

The influence of shorter cycle lengths when the corridor was in an optimized state was assessed using the WaySync-D suite functionalities. Variable levels were isolated using Websters Formula for Optimal Cycle Lengths and evaluated 70 to 110 second cycle lengths. Close inspection of all turning maneuvers and directions of travel helped realize the notable findings when assessing the impact of shorter cycle lengths. It was found that along the corridor of interest during the peak-period there occurs a point where improvements begin to become most recognizable, and diminishing returns were observed beyond this point. This occurred when assessing 90 second cycle length models, the midpoint of all five cycle lengths that were evaluated. Southbound through movements, experienced a stop delay decrease from 4.5 seconds to 2.3 seconds. For vehicles on the Northbound approach, through movements reduced from a LOS E to a LOS D when evaluating the transition to a 90 second cycle length. Eastbound left and right turning maneuvers had a 50% decrease in delay when evaluating the change from a 100 second cycle length down to a 90 second cycle length. In this scenario, although the smallest cycle length had the largest impact on delay reduction the change was small in comparison to that of the 90 second adjustment. This finding indicates that shorter cycle lengths do impact

vehicle delays and stop delays on all approaches, but the benefit become less noticeable at a 90 second threshold during the PM-peak.

The addition of LPI timings at the Crown Zellerbach intersection in the non-optimized and optimized models revealed that consideration must be placed on the different directions of travel. In the Northbound direction, a 7 second LPI was found to be the best option given the consistent vehicle delay and stop delay as long as the corridor is in an optimized state. In scenarios where a non-optimized corridor was evaluated, using a 7 second LPI resulted in much larger delay and stop delay as compared to the 3- and 5 second models. Evaluation of the Eastbound direction of travel revealed an opposite effect, where the non-optimized conditions performed better when implementing an LPI of any duration. Increases in both delay and number of stops were observed which became more significant as the length of the LPI increased. This finding indicates that there may be a tradeoff when selecting to implement an LPI along the minor approach, as it will cost an increase in delay for vehicles. The weight of this tradeoff must be compared to the pedestrian safety improvements to most accurately assess if an LPI is suitable along the minor street approach.

6.2 LIMITATIONS

One important consideration when using HILS is that the physical signal controllers present a limiting factor when running multiple simulation trials, as is required by current agency practice. In traditional microsimulation modeling, PTV VISSIM can be run at an accelerated rate, allowing many hours and data to be simulated in a short period of time, but HILS requires the simulation to be run in real-time. This limitation is one consideration when selecting this study design as the number of simulation runs were restricted due to the length of each simulated run. Due to synchronization of all software packaged used in this study, restrictions for implementing LPIs were also present. Although PTV VISSIM permits this functionality, the current version of PASS used did not have this capability. For this reason, a workaround was found using Maxtime but LPIs were only assessed at the Crown Zellerbach location due to limitations in the various required software packages.

6.3 FUTURE WORK

Next steps to advance this work include identifying how the knowledge retained can be best applied by the agency at additional locations. Documenting frequently asked questions and procedural steps in the process to better operationalize this HILS study design is one short term goal. that the research would be advanced by testing a longer corridor design with highly saturated conditions in both directions, as these conditions are expected to produce different optimization concerns. Another characteristic for future sites would be those that frequently require vehicles to perform more than one stop at a given intersection.

A secondary site includes one that features an as-built transit signal priority system along the corridor. These conditions will change the optimization parameter and would have to consider other phases at certain instances along the corridor.

Lastly, corridors with consistently high multimodal volumes may be a next step towards fully understanding LPI implementation across multiple intersections. These are three avenues of

examples of studies that would help better understand locational considerations and the applicability of this HILS study design at a larger scale so deployment across the State can be focused towards specific improvements.

7.0 REFERENCES

Abdelgawad, H., Rezaee, K., El-Tantawy, S., Abdulhai, B., & Abdulazim, T. (2015). Assessment of Adaptive Traffic Signal Control Using Hardware in the Loop Simulation. *IEEE Conference on Intelligent Transportation Systems, Proceedings, ITSC*, *2015-October*, 1189–1195. https://doi.org/10.1109/ITSC.2015.196

Byrne, N., Koonce, P., Bertini, R. L., Pangilinan, C., Lasky, M., Byrne, N., Bertini, R. L., & Pangilinan, C. (2005). Using Hardware-in-the-Loop Simulation to Evaluate Signal Control Strategies for Transit Signal Priority. In *Transportation Research Record: Journal of the Transportation Research Board*.

De Villa, A.R., Casas, J., Breen, M., Perarnau, J. 2014. Static OD Estimation Minimizing the Relative Error and the GEH Index. *Procedia-Social and Behavioral Sciences.* Vol. 111. pp. 810-818.

Engelbrecht, R. (2001). Using Hardware-in-the-Loop Traffic Simulation to Evaluate Traffic Signal Controller Features. 27th Annual Conference of the IEEE Industrial Electronics Society. Denver, CO. 10.1109/IECON.2001.975584

Feldman, O. 2012. The GEH Measure and Quality of the Highway Assignment Models. *Association for European Transport and Contributors 2012.* pp. 1-18.

FHWA (Federal Highway Administration). (2022). Signal Timing Tool Box. Signal Timing on a Shoestring. United States Department of Transportation.

FHWA. (2020). Automated Traffic Signal Performance Measures. US Department of Transportation. https://ops.fhwa.dot.gov/publications/fhwahop20002/ch2.htm.

Highway Capacity Manual (HCM), National Academies of Sciences, Engineering, and Medicine. 2022. *Highway Capacity Manual 7th Edition: A Guide for Multimodal Mobility Analysis*. Washington, DC: The National Academies Press. https://doi.org/10.17226/26432.

Hunter, P.M. Roe, M. Wu, S.K. (2010). Hardware-in-the-Loop Simulation Evaluation of Adaptive Control. Transportation Research Record, 2192(1). 167-176. https://doi.org/10.3141/2192-16

Jones, S.L. Sullivan, A.J. Cheekoti, N. Anderson, M.D. Malave, D. (2004). Traffic Simulation Software Comparison Study. University Transportation Center for Alabama Report 02217.

Koonce, P. Rodegerdts, L. (2008). Traffic Signal Timing Manual. Rep No. FHWA-HOP-08-024. Washington, D.C.

Koonce, P. Urbanik, T. Bullock, D. (1999). Evaluation of Diamond Interchange Signal Controller Settings by Using Hardware-in-the-Loop Simulation. Transportation Research Record. 59-66.

Li, P. Mirchandani, P.B. (2016). A New Hardware-in-the-Loop Traffic Signal Simulation Framework to Bridge Traffic Signal Research and Practice. IEEE Transactions on Intelligent Transportation Systems, 17(9). 2430-2439. 10.1109/TITS.2016.2523443

Marnell, P., Zebell, P., Koonce, P., & Quayle, S. (2017). Evaluating transit priority signal phasing at most multimodal intersection in Portland, Oregon. *Transportation Research Record*, *2619*, 44–54. https://doi.org/10.3141/2619-05

NACTO (National Association of City Transportation Officials). (2013). Urban Street Design Guide. Island Press. p. 250

Oregon Department of Transportation (ODOT). (2025). Planning & Technical Guidance - Signalized Intersection Controls. https://www.oregon.gov/odot/planning/pages/technical-tools.aspx

Oregon Department of Transportation (ODOT). 2011. Protocol for VISSIM Simulation. *ODOT VISSIM Protocol.* Salem, OR.

PBOT (Portland Bureau of Transportation). (2024). Pedestrian Head Starts. City of Portland. https://www.portland.gov/transportation/traffic-operations/pedestrian-head-starts

PTV AG. 2018. PTV VISSIM 11 User Manual. *PTV Group.* Karlsruhe, Germany.

Q-Free. 2024. 2070LDX Controller. *Traffic Management Solutions.*

Stevanovic, A. Abdel-Rahim, A. Zlatkovic, M. Amin, E. (2009). Microscopic Modeling of Traffic Signal Operations: Comparative Evaluation of Hardware-in-the-Loop and Software-in-the-Loop Simulations. Transportation Research Record, 2128(1). 143-151. https://doi.org/10.3141/2128-15

Wang, D., Tian, Z., & Yang, G. (2019). Virtual Controller Interface Device for Hardware-in-the-Loop Simulation of Traffic Signals. IEEE Intelligent Transportation Systems Magazine, 13(2), 201–216. https://doi.org/10.1109/MITS.2019.2898968

Wang, G. (2020). Measuring the Quality of Arterial Traffic Signal Timing – A Trajectory-based Methodology. University of Nevada, Reno.

Wang, D., Tian, Z., Gholami, A., & Yang, G. (2021). Evaluation of virtual controller interface device and software-in-the-loop simulation. Proceedings of the Institution of Civil Engineers: Transport, 174(6), 367–377. https://doi.org/10.1680/jtran.17.00149

Yun, I., Best, M., & Park, B. (2007). Evaluation of adaptive maximum feature in actuated traffic controller: Hardware-in-the-loop simulation. Transportation Research Record, 2035, 134–140. https://doi.org/10.3141/2035-15

APPENDIX A

Table 14. GEH Statistics VISSIM

Street	Time	NB Left	NB Through	NB Right	EB Left	EB Through	EB Right	SB Left	SB Through	SB Right	WB Left	WB Through	WB Right
Walnut	1630-1645	0.0	0.1	0.7	0.4	1.2	0.9	0.8	1.7	0.5	2.1	0.8	1.9
Walnut	1645-1700	0.5	2.2	1.4	0.8	0.0	0.8	0.0	0.2	0.4	0.4	0.0	1.2
Walnut	1700-1715	1.6	0.1	0.9	0.9	0.0	0.0	1.5	0.3	1.8	2.0	1.4	0.3
Walnut	1715-1730	1.8	0.4	0.0	0.4	0.8	1.4	1.5	2.3	1.9	3.0	1.4	0.3
Watts	1630-1645	2.4	0.7		0.5		0.8	0.0	2.2	0.7			
Watts	1645-1700	0.0	1.2		1.1		0.3	0.0	0.4	1.0			
Watts	1700-1715	0.4	1.9		0.0		2.3	0.0	1.3	1.1			
Watts	1715-1730	1.7	1.2		0.3		0.6	0.0	2.6	3.8			
Maple	1630-1645	0.4	1.7	0.4	0.3	0.5	1.2	1.0	1.9	2.5	1.2	1.2	1.0
Maple	1645-1700	0.5	1.3	1.9	0.3	0.0	0.0	0.0	1.0	0.5	0.3	1.2	0.4
Maple	1700-1715	0.5	0.9	0.0	0.3	2.0	0.4	0.7	2.1	1.3	0.6	0.0	1.6
Maple	1715-1730	0.0	3.1	0.7	1.2	0.8	0.0	0.3	3.5	2.8	1.5	0.9	1.6
Columbia	1630-1645	0.0	0.0	0.1				0.8	0.1	0.2	0.2	0.2	0.5
Columbia	1645-1700	0.1	0.1	0.0				1.0	0.1	0.3	0.1	0.2	0.0
Columbia	1700-1715	0.1	0.1	0.2				0.7	0.0	0.0	0.1	0.1	0.2
Columbia	1715-1730	0.2	0.2	0.0				0.8	0.1	0.7	0.1	0.1	0.0
Crown	1630-1645	0.2	1.1	1.4	1.2	0.5	0.5	0.8	1.4	1.2	1.3	1.3	1.7
Crown	1645-1700	0.5	0.6	0.3	0.5	1.2	0.7	0.3	0.9	1.8	0.0	1.4	0.5
Crown	1700-1715	1.0	3.9	0.3	0.9	1.4	1.0	0.3	1.1	2.0	1.5	1.4	0.2
Crown	1715-1730	0.9	2.3	0.7	0.5	0.6	1.5	0.3	3.2	0.5	1.8	0.6	2.3

Note: GEH=Geoffrey E Havers values, NB=Northbound Approach, EB=Eastbound Approach, SB=Southbound Approach, WB=Westbound Approach.

Table 15. Vehicular Delay with HILS

Street	Time	NB Left	NB Through	NB Right	EB Left	EB Through	EB Right	SB Left	SB Through	SB Right	WB Left	WB Through	WB Right
Walnut	1630-1645	12.5	3.7	0.8	62.2	0	8.3	26.2	0.8	0.1	60.7	73.1	11.6
Walnut	1645-1700	0	4.1	0.3	61	0	9.2	19.6	0.8	0.9	45.9	50.5	13.2
Walnut	1700-1715	10.9	3.5	0.6	86.8	0	38.5	19.4	0.8	2.7	58.2	58.3	9.5
Walnut	1715-1730	0.6	3.8	0	70.3	0	13	22.7	0.8	1.8	65	68.8	11.3
Watts	1630-1645	65.2	2.2		470.1		343.4		2.6	3.6			
Watts	1645-1700		2.1		498.6		391.2		2.1	2.5			
Watts	1700-1715	116.9	2.4		507.1		372.9		2.5	3.4			
Watts	1715-1730	30.1	1.9		511.6		418.6		2.6	1.5			
Maple	1630-1645	0.5	3	0.2	63.3	72	16.8	19.7	4.1	6.5	77.1	5.2	11.9
Maple	1645-1700		3.3	0	95.2	86.9	26.1	19.3	4.8	1.5	48.9	5.3	13.3
Maple	1700-1715	0.4	2.6	1.5	104.9	110.2	12.9	19.6	4.8	5	71.8	4.7	10.7
Maple	1715-1730		3.4	0.4	95.5	99.3	28.6	20	4.7	1.9	60.9	4.6	11
Columbia	1630-1645	9.8	7.6	0.2				16	5.1	6.7	221.8	132.8	104.6
Columbia	1645-1700	17.9	7.6	4.7				13.7	5.9	7.2	299.9	195.1	138.2
Columbia	1700-1715	18.4	7.2	2.3				21.3	7.5	5.8	307.8	194.6	154.3
Columbia	1715-1730		7.6	2.4				12.2	5.9	5.2	294.1	131.7	124
Crown	1630-1645	54.1	8.3	0	58.7	62.1	11.3	88.9	4.5	2.6	55.3	61.8	24.1
Crown	1645-1700	50.8	8.5	0.8	45.2	48.7	10.8	79.8	4.7	1.2	56.7	70.8	37
Crown	1700-1715	54.6	8.2	0.6	57.1	58.9	11.6	71.3	5.6	4.7	49.4	32	21.5
Crown	1715-1730	61.2	8.7	0	46	84.1	12.5	68.2	4.9	1.7	50.1	78	43.4

Key: yellow=LOS A, orange=LOS B, light green=LOS C, green=LOS D, dark red=LOS E, blue=LOS F.
Note: HILS= hardware-in-the-loop simulation, NB=Northbound Approach, EB=Eastbound Approach, SB=Southbound Approach, WB=Westbound Approach.

Table 16. Average Maximum Queue Length using HILS

Street	Time	NB Left	NB Through	NB Right	EB Left	EB Through	EB Right	EB Left	EB Through	EB Right	WB Left	WB Through	WB Right
Walnut	1630-1645	0	318.4	0	48.8	48.8	25.3	46	45.9	67	71.9	71.9	83.4
Walnut	1645-1700	0	296.7	0	64	64	39.1	52.2	67.8	88.8	66.6	66.6	57.4
Walnut	1700-1715	8.7	262.6	0	115.8	115.8	37	94.7	52.4	73.5	79.4	79.4	51.5
Walnut	1715-1730	0	308.7	0	84.3	84.3	39	73.9	62.3	83.3	56.9	56.9	77.4
Watts	1630-1645	13.8	207.3		572.8		589.3		106.3	123.5			
Watts	1645-1700	0	187.6		590.2		606.7		109.6	126.9			
Watts	1700-1715	8.5	227.8		577.6		594.1		114.7	132			
Watts	1715-1730	17.2	148.4		577.3		593.8		112.4	129.7			
Maple	1630-1645	0	177	0	107.3	107.3	48	18.3	187.3	200.6	100.8	0	42.8
Maple	1645-1700	0	175.3	0	135.7	135.7	50.6	15.3	238	251.4	70.4	0	62.7
Maple	1700-1715	0	153.5	26.4	182.9	182.9	37.4	42.7	223	236.4	90.5	0	54.5
Maple	1715-1730	0	267.2	0	151.3	151.3	46	18.8	260.6	273.9	94.8	0	44.9
Columbia	1630-1645	22.6	585.5	0				28.3	140.1	155.5	403	56.7	83.5
Columbia	1645-1700	13.5	587.3	37.8				38.2	169.3	184.6	480.6	216.2	243
Columbia	1700-1715	0	593.1	0				17	196.1	211.5	410.8	213.1	239.9
Columbia	1715-1730	0	565.3	0				15.8	178.5	193.8	472.1	180.5	207.2
Crown	1630-1645	61.3	744.9	0	27.7	19.3	110.3	95.8	105.1	49.2	57.6	90.7	113.4
Crown	1645-1700	66.4	783	21.3	21.2	29.3	86	49	137.6	0	69.1	90.6	113.3
Crown	1700-1715	61.8	773.3	21.2	51.2	20.9	97.9	80	152.5	40.9	35.9	53.4	76.1
Crown	1715-1730	78.8	584.5	0	44.1	38.3	94.1	65.9	137.4	13.7	39.1	103.9	126.6

Key: ■orange = delay 200 < Q < 300 seconds, ■red = Q > 300 seconds

Note: HILS= hardware-in-the-loop simulation, NB=Northbound Approach, EB=Eastbound Approach, SB=Southbound Approach, WB=Westbound Approach.

Table 17. Number of Stops using HILS

Street	Time	NB Left	NB Through	NB Right	EB Left	EB Through	EB Right	EB Left	EB Through	EB Right	WB Left	WB Through	WB Right
Walnut	1630-1645	0.5	0.2	0	1.4	0	1.2	1.1	0	0	1	1.5	1.2
Walnut	1645-1700	0	0.2	0	1.4	0	1.3	1	0	0	1	1	1.5
Walnut	1700-1715	1	0.2	0	2	0	1.5	0.9	0	0.2	1.2	1	1.2
Walnut	1715-1730	0	0.2	0	1.4	0	0.9	1.2	0	0.2	1.2	1.2	1.5
Watts	1630-1645	1	0.1		5		5		0.1	0.3			
Watts	1645-1700	0	0.1		5.2		5.6		0.1	0.2			
Watts	1700-1715	1	0.1		5.2		5.8		0.1	0.3			
Watts	1715-1730	1	0.1		5.1		5		0.1	0.1			
Maple	1630-1645	0	0.1	0	1.1	1	1.4	0.8	0.3	0.5	1.1	0.9	1.5
Maple	1645-1700	0	0.1	0	1.3	1.2	1.5	0.6	0.3	0.1	0.9	1	1.6
Maple	1700-1715	0	0.1	0.1	1.4	1.5	1.4	0.8	0.3	0.4	1	0.8	1.3
Maple	1715-1730	0	0.1	0	1.3	1.4	1.7	0.8	0.3	0.2	0.9	0.9	1.6
Columbia	1630-1645	0.5	0.3	0				0.7	0.2	0.3	2.4	1.7	2.5
Columbia	1645-1700	1	0.3	0.3				0.6	0.3	0.4	3.1	3	3.4
Columbia	1700-1715	0.5	0.3	0.2				0.6	0.3	0.3	3.3	3	3.1
Columbia	1715-1730		0.4	0.1				0.6	0.3	0.4	3.1	2	2.9
Crown	1630-1645	1	0.5	0	1	0.9	1	1.2	0.2	0.2	1	1	1.6
Crown	1645-1700	1.1	0.5	0	0.8	0.8	1	1	0.2	0	0.9	1.1	1.8
Crown	1700-1715	1	0.5	0	0.9	1	1.1	1	0.2	0.3	0.7	0.8	1.6
Crown	1715-1730	1.1	0.5	0	0.8	1.1	1.1	1	0.2	0.1	0.8	1.2	1.8

Key: ■red = Stops > 1

Note: HILS= hardware-in-the-loop simulation, NB=Northbound Approach, EB=Eastbound Approach, SB=Southbound Approach, WB=Westbound Approach.

Table 18. Stop Delay using HILS

Street	Time	NB Left	NB Through	NB Right	EB Left	EB Through	EB Right	EB Left	EB Through	EB Right	WB Left	WB Through	WB Right
Walnut	1630-1645	4.9	1.4	0	53.7		0.2	17.3	0.2	0	55.7	67.3	4.3
Walnut	1645-1700		1.6	0	52.9		0.3	11.5	0.2	0	40.9	45.3	5.3
Walnut	1700-1715	3.5	1.2	0	76.7		28.8	12.7	0.3	0.4	52.7	53.3	2.6
Walnut	1715-1730	0	1.5	0	62		4.8	13.6	0.2	0.2	59.4	63.8	2.5
Watts	1630-1645	52.7	0.5		435.4		308.6		0.7	1.1			
Watts	1645-1700		0.4		462		353.6		0.5	0.6			
Watts	1700-1715	108.8	0.6		471.2		335.7		0.6	0.6			
Watts	1715-1730	21.4	0.4		474.6		377.2		0.8	0.3			
Maple	1630-1645	0	1.3	0	55.7	64.8	6.8	13.6	0.8	1.1	70.7	0.2	4.5
Maple	1645-1700		1.4	0	86.3	77.5	14.9	13.4	1	0.3	43.7	0.1	5.8
Maple	1700-1715	0	1	0	94.3	99.4	4.2	13.4	0.8	0.7	65.7	0.1	3.2
Maple	1715-1730		1.4	0	85.4	89.3	16.8	12.5	0.9	0	55.6	0.1	3.5
Columbia	1630-1645	1.7	3.8	0				8.9	2.3	2.7	203.3	119.9	87.9
Columbia	1645-1700	5.4	4.1	0.1				6.2	2.8	3.8	275.3	173	114
Columbia	1700-1715	8.9	3.8	1.1				12.7	3.9	2.4	282	171.3	131.7
Columbia	1715-1730		3.9	0.1				6.6	3	1.6	269.9	116.3	104.2
Crown	1630-1645	43.8	3.1	0	48.3	51.9	0.2	75.5	1.5	0	45.9	52.4	11.4
Crown	1645-1700	41.2	3.4	0	35.2	39	0.3	67.4	1.5	0	47.3	61.6	23
Crown	1700-1715	44.8	3.3	0	46.9	48.4	0.2	58.5	2	0	42.1	23.8	9.8
Crown	1715-1730	50.3	3.4	0	36.9	72.8	0.6	56.6	1.6	0	41.4	67.4	27.8

Key: ■dark red = Stop delay > 30s

Note: HILS= hardware-in-the-loop simulation, NB=Northbound Approach, EB=Eastbound Approach, SB=Southbound Approach, WB=Westbound Approach.

APPENDIX B

Table 19. PM Average Max Queue Length (feet)

Approach Direction	Walnut Non Opt	Walnut Opt	Watts Non Opt	Watts Opt	Maple Non Opt	Maple Opt	Columbia Non Opt	Columbia Opt	Crown Non Opt	Crown Opt
NBT	334.5	402.8	489.3	353.4	477.9	340.4	315.5	288.8	1003.2	1138.2
NBL	0.0	0.0	4.4	4.4	4.5	5.0	0.0	0.0	38.7	38.8
NBR	10.4	9.1			13.9	21.2	0.0	12.4	15.3	22.7
SBT	91.5	306.9	130.7	149.4	180.9	225.8	215.4	159.5	168.9	149.9
SBL	68.9	79.2			53.8	42.1	10.0	22.6	131.2	145.7
SBR	116.8	332.2	147.9	166.7	194.3	239.1	230.8	174.9	25.2	13.5
EBT	76.0	72.5			210.4	230.0			31.2	32.5
EBL	76.0	72.5	580.7	457.0	210.4	230.0			40.8	47.8
EBR	44.4	44.1	597.2	362.5	49.3	75.5			86.8	81.8
WBT	91.2	87.2			64.9	59.4	391.7	430.5	96.1	131.4
WBL	91.2	87.2			96.7	87.3	519.8	543.6	118.8	154.16
WBR	63.4	63.5			63.8	58.3	418.5	457.3	70.7	73.6

Table 20. PM Average Vehicle Delay (seconds)

Approach Direction	Walnut Non Opt	Walnut Opt	Watts Non Opt	Watts Opt	Maple Non Opt	Maple Opt	Columbia Non Opt	Columbia Opt	Crown Non Opt	Crown Opt
NBT	4.0	4.8	4.6	4.5	4.6	4.6	3.0	4.9	7.6	9.7
NBL	10.0	2.3	108.2	79.7	15.5	10.2	10.8	7.6	56	104.6
NBR	5.9	4.5			1.4	2.2	1.2	2.8	2.9	4.2
SBT	2.0	6.3	1.3	2.9	3.2	4.2	3.5	3.2	5.3	4.2
SBL	25.8	29.5			23.8	14.2	20.7	16.2	102.1	145.1
SBR	2.0	6.3	2.0	2.2	2.7	5.4	4.2	3.0	2.4	2.0
EBT	62.5	75.4			168.8	224.7			63.4	69.5
EBL	88.7	78.9	541.1	383.4	155.4	210.0			46.3	61.7
EBR	11.0	9.3	415.1	259.8	33.4	103.0			11.1	11.2
WBT	61.1	58.4			18.9	14.5	284.9	309.3	55.5	104.8
WBL	73.1	75.1			82.6	70.9	397.2	449.9	48.0	62.2
WBR	13.1	12.0			20.1	13.0	246.5	252.6	43.8	71.1

Table 21. PM Average Stop Delay (seconds)

Approach Direction	Walnut Non Opt	Walnut Opt	Watts Non Opt	Watts Opt	Maple Non Opt	Maple Opt	Columbia Non Opt	Columbia Opt	Crown Non Opt	Crown Opt
NBT	1.6	2.1	1.0	2.1	1.4	2.2	0.4	2.7	4.1	5.1
NBL	5.5	0.0	97.9	71.4	5.6	2.8	1.4	4.1	45.8	94.2
NBR	0.0	0.0			0.0	0.0	0.2	0.7	0.0	0.1
SBT	0.6	2.3	0.3	0.9	1.3	1.2	1.4	1.4	1.7	1.4
SBL	17.1	19.4			15.7	8.0	14.5	10.6	87.7	128.9
SBR	0.3	1.7	0.4	0.5	0.7	1.7	1.4	0.9	0.0	0.0
EBT	54.3	67.2			156.0	208.4			53.2	59.6
EBL	79.5	70.2	508.3	358.8	143.1	194.2			37.3	51.8
EBR	2.1	1.4	375.9	234.9	21.7	85.8			0.4	0.4
WBT	55.8	52.9			11.7	7.5	261.6	283.7	43.3	90.3
WBL	66.7	69.1			76.4	65.2	370.0	419.4	28.3	52.8
WBR	4.9	4.1			12.3	5.5	219.9	224.6	38.7	52.1

Table 22. PM Average Number of Stops

Approach Direction	Walnut Non Opt	Walnut Opt	Watts Non Opt	Watts Opt	Maple Non Opt	Maple Opt	Columbia Non Opt	Columbia Opt	Crown Non Opt	Crown Opt
NBT	0.2	0.2	0.2	0.2	0.2	0.2	0.1	0.2	0.3	0.5
NBL	0.3	0.0	1.0	1.0	0.8	0.5	0.8	0.3	1	1.0
NBR	0.3	0.1			0.1	0.2	0.0	0.2	0.3	0.4
SBT	0.1	0.3	0.1	0.2	0.1	0.2	0.2	0.2	0.2	0.2
SBL	1.1	1.1			1.0	0.6	0.7	0.6	1.3	1.5
SBR	0.2	0.3	0.1	0.1	0.1	0.3	0.2	0.2	0.1	0.1
EBT	1.4	1.5			1.8	2.2			1.0	0.9
EBL	1.8	1.6	4.6	3.5	1.6	2.2			0.8	0.9
EBR	1.3	1.1	5.0	3.8	1.6	2.4			1.0	1.0
WBT	1.2	1.2			1.4	1.5	3.0	3.2	1.3	1.7
WBL	1.2	1.2			1.1	1.0	3.5	3.9	2.0	2.4
WBR	1.5	1.5			1.5	1.4	3.7	3.8	0.9	0.9

Table 23. AM Average Max Queue Length (feet)

Approach Direction	Walnut Non Opt	Walnut Opt	Watts Non Opt	Watts Opt	Maple Non Opt	Maple Opt	Columbia Non Opt	Columbia Opt	Crown Non Opt	Crown Opt
NBT	153.5	173.5	101.9	99.3	123.4	167.2	262.0	226.2	328.1	495.9
NBL	0.0	0.0	7.3	23.2	0.0	0.0	2.1	2.1	38.9	34.2
NBR	27.2	22.1			0.0	4.8	23.0	13.6	13.8	24.5
SBT	68.9	99.2	146.8	95.8	497.8	102.3	441.9	449.0	234.8	228.4
SBL	70.5	59.0			16.9	12.3	21.5	13.3	107.5	91.2
SBR	94.2	124.5	164.0	113.1	511.2	115.7	457.3	464.4	8.8	6.9
EBT	75.9	77.1			98.7	96.7			29.7	23.6
EBL	75.9	77.1	138.0	178.7	98.7	96.7			51.4	47.8
EBR	53.8	61.8	65.0	104.7	41.0	39.4			101.2	99.9
WBT	146.6	146.9			56.3	61.0	33.1	28.8	81.6	65.7
WBL	146.6	146.9			89.7	78.2	19.4	22.8	104.4	88.4
WBR	71.4	69.0			55.1	59.9	59.9	55.6	68.0	61.1

Table 24. AM Average Vehicle Delay (seconds)

Approach Direction	Walnut Non Opt	Walnut Opt	Watts Non Opt	Watts Opt	Maple Non Opt	Maple Opt	Columbia Non Opt	Columbia Opt	Crown Non Opt	Crown Opt
NBT	2.8	3.8	1.4	1.3	2.7	3.4	5.0	5.5	5.8	13.6
NBL	1.0	5.1	102.6	55.8	10.3	7.6	4.9	7.2	85.2	76.5
NBR	4.4	4.9			0.7	2.3	5.6	5.4	3.5	5.6
SBT	1.1	2.2	1.8	0.7	5.6	1.0	9.5	8.1	5.9	5.9
SBL	6.7	7.0			9.8	3.6	10.5	13.0	90.0	85.1
SBR	0.8	1.0	2.8	0.7	4.3	1.6	5.0	5.2	2.6	2.5
EBT	64.0	68.1			71.7	75.0			61.9	55.3
EBL	60.7	63.5	82.0	102.9	68.9	69.8			47.0	52.0
EBR	11.4	11.4	18.0	37.5	14.4	13.4			12.8	12.7
WBT	98.3	104.0			9.2	9.1	46.7	29	73.5	48.5
WBL	99.5	103.4			69.2	70.2	40.7	51.8	52.4	52.1
WBR	10.5	7.7			8.1	8.7	10.5	10.5	27.3	19.9

Table 25. AM Average Stop Delay (seconds)

Approach Direction	Walnut Non Opt	Walnut Opt	Watts Non Opt	Watts Opt	Maple Non Opt	Maple Opt	Columbia Non Opt	Columbia Opt	Crown Non Opt	Crown Opt
NBT	1.0	1.6	0.2	0.3	1.1	1.5	2.4	2.9	1.8	7.1
NBL	0.0	2.5	89.6	43.9	5.9	3.2	0.6	0.1	74.7	67.8
NBR	0.2	0.1			0.0	0.0	0.1	0.1	0.0	0.1
SBT	0.3	0.7	0.5	0.1	0.5	0.3	5.0	3.3	1.9	1.9
SBL	1.6	1.8			2.7	0.9	4.1	4.9	75.9	72.2
SBR	0.1	0.2	0.9	0.1	0.2	0.5	1.8	1.9	0.0	0.0
EBT	56.4	59.8			63.9	67.3			52.3	46.2
EBL	51.9	54.9	75.1	94.2	61.3	62.0			37.0	42.1
EBR	2.8	2.6	9.2	26.6	4.9	4.3			0.9	1.0
WBT	89.8	95.0			2.0	2.0	40.9	24.1	62.4	38.2
WBL	89.6	93.2			62.8	64.5	35.9	45.7	14.6	8.6
WBR	3.4	0.9			1.1	1.5	2.4	2.2	43.2	43.2

Table 26. AM Average Number of Stops

Approach Direction	Walnut Non Opt	Walnut Opt	Watts Non Opt	Watts Opt	Maple Non Opt	Maple Opt	Columbia Non Opt	Columbia Opt	Crown Non Opt	Crown Opt
NBT	0.1	0.2	0.1	0.1	0.1	0.2	0.2	0.3	0.4	0.6
NBL	0.0	0.2	1.5	1.2	0.5	0.5	0.5	0.5	1.0	0.8
NBR	0.3	0.4			0.0	0.2	0.4	0.4	0.1	0.4
SBT	0.1	0.1	0.1	0.0	0.3	0.0	0.4	0.5	0.2	0.2
SBL	0.3	0.4			0.5	0.2	0.5	0.7	1.2	1.1
SBR	0.0	0.0	0.2	0.0	0.1	0.1	0.2	0.3	0.1	0.2
EBT	1.4	1.3			1.0	1.1			1.0	0.9
EBL	1.5	1.5	1.2	1.4	1.0	1.0			0.9	0.9
EBR	1.2	1.3	1.6	1.8	1.5	1.5			1.2	1.1
WBT	1.5	1.4			1.3	1.3	0.9	0.7	1.3	1.1
WBL	1.8	1.8			1.1	1.0	0.7	0.9	1.6	1.4
WBR	1.2	1.2			1.3	1.3	1.2	1.3	0.9	0.9

Table 27. NBT Performance at Shorter Cycle Lengths

Row Labels	Queue Length	Vehicle Delay	Stop Delay	Stops
1 Walnut NBT 70s	400.4	6.4	2.3	0.3
2 Watts NBT 70s	410.4	6.0	1.5	0.3
3 Maple NBT 70s	529.4	9.7	4.8	0.4
4 Colombia NBT 70s	703.0	11.5	4.6	0.7
5 Crown NBT 70s	173.3	4.4	2.4	0.1
1 Walnut NBT 80s	335.8	4.8	1.5	0.2
2 Watts NBT 80s	309.7	4.2	1.0	0.2
3 Maple NBT 80s	565.3	9.5	5.0	0.4
4 Colombia NBT 80s	774.2	13.8	7.6	0.6
5 Crown NBT 80s	79.3	1.3	0.5	0.0
1 Walnut NBT 90s	357.7	4.5	1.4	0.2
2 Watts NBT 90s	186.7	2.2	0.5	0.1
3 Maple NBT 90s	614.1	9.5	4.3	0.5
4 Colombia NBT 90s	229.4	4.3	2.3	0.2
5 Crown NBT 90s	149.0	2.1	0.9	0.1
1 Walnut NBT 100s	330.7	4.3	1.4	0.2
2 Watts NBT 100s	263.3	3.1	0.5	0.1
3 Maple NBT 100s	325.8	4.4	1.8	0.2
4 Colombia NBT 100s	417.8	8.3	4.5	0.4
5 Crown NBT 100s	358.4	3.5	0.3	0.1
1 Walnut NBT 110s	352.7	4.6	1.6	0.2
2 Watts NBT 110s	257.8	3.0	0.5	0.1
3 Maple NBT 110s	328.6	4.3	1.8	0.2
4 Colombia NBT 110s	403.2	6.9	3.3	0.4
5 Crown NBT 110s	974.5	8.0	2.8	0.4

Note: NBT= northbound through

Table 28. NBL Performance at Shorter Cycle Lengths

Row Labels	Queue Length	Vehicle Delay	Stop Delay	Stops
1 Walnut NBL 70s	2.2	6.3	1.1	0.3
2 Watts NBL 70s	4.3	30.1	22.1	1.0
3 Maple NBL 70s	0.0	9.9	0.2	0.3
4 Colombia NBL 70s	4.4	10.2	2.1	0.5
5 Crown NBL 70s	44.2	19.2	9.7	0.8
1 Walnut NBL 80s	0.0	9.9	1.8	0.7
2 Watts NBL 80s	4.3	61.4	53.3	1.0
3 Maple NBL 80s	3.2	4.5	2.2	0.3
4 Colombia NBL 80s	2.2	8.9	1.9	0.3
5 Crown NBL 80s	45.9	34.2	23.4	0.9
1 Walnut NBL 90s	0.0	0.4	0.0	0.0
2 Watts NBL 90s	4.4	37.7	29.6	1.0
3 Maple NBL 90s	0.0	7.7	1.8	0.5
4 Colombia NBL 90s	6.6	12.4	2.4	0.7
5 Crown NBL 90s	55.9	36.4	25.8	0.9
1 Walnut NBL 100s	5.1	15.3	6.9	0.7
2 Watts NBL 100s	6.5	65.9	57.7	1.0
3 Maple NBL 100s	0.0	6.8	0.2	0.5
4 Colombia NBL 100s	6.8	18.1	8.0	0.6
5 Crown NBL 100s	55.4	47.0	36.2	1.0
1 Walnut NBL 110s	4.4	13.9	4.3	0.8
2 Watts NBL 110s	11.6	49.4	39.1	1.0
3 Maple NBL 110s	5.1	10.6	3.8	0.5
4 Colombia NBL 110s	3.4	11.0	0.0	0.0
5 Crown NBL 110s	37.8	62.9	52.8	1.0

Table 29. NBR Performance at Shorter Cycle Lengths

Row Labels	Queue Length	Vehicle Delay	Stop Delay	Stops
1 Walnut NBR 70s	4.5	1.5	0.0	0.1
3 Maple NBR 70s	17.4	2.7	0.1	0.2
4 Colombia NBR 70s	9.6	5.6	1.2	0.2
5 Crown NBR 70s	15.2	3.0	0.0	0.3
1 Walnut NBR 80s	4.6	6.0	2.0	0.4
3 Maple NBR 80s	36.2	5.5	0.1	0.4
4 Colombia NBR 80s	23.5	7.9	3.2	0.4
5 Crown NBR 80s	0.0	0.1	0.0	0.0
1 Walnut NBR 90s	0.0	3.4	1.6	0.1
3 Maple NBR 90s	15.7	2.8	0.0	0.1
4 Colombia NBR 90s	9.5	2.5	1.2	0.1
5 Crown NBR 90s	0.0	0.1	0.0	0.0
1 Walnut NBR 100s	0.0	0.3	0.0	0.0
3 Maple NBR 100s	7.3	3.1	0.0	0.3
4 Colombia NBR 100s	15.4	2.9	0.0	0.2
5 Crown NBR 100s	0.0	0.3	0.0	0.0
1 Walnut NBR 110s	4.6	2.2	0.0	0.0
3 Maple NBR 110s	0.0	0.4	0.0	0.0
4 Colombia NBR 110s	20.1	3.2	0.6	0.2
5 Crown NBR 110s	13.1	1.6	0.0	0.0

Table 30. SBT Performance at Shorter Cycle Lengths

Row Labels	Queue Length	Vehicle Delay	Stop Delay	Stops
1 Walnut SBT 70s	44.5	0.8	0.1	0.0
2 Watts SBT 70s	112.8	1.6	0.3	0.1
3 Maple SBT 70s	297.0	7.9	1.2	0.5
4 Colombia SBT 70s	92.4	3.3	0.6	0.1
5 Crown SBT 70s	181.2	8.6	2.8	0.3
1 Walnut SBT 80s	55.2	1.2	0.3	0.0
2 Watts SBT 80s	88.7	0.8	0.1	0.0
3 Maple SBT 80s	318.5	8.7	2.3	0.6
4 Colombia SBT 80s	245.3	5.7	0.9	0.2
5 Crown SBT 80s	180.2	7.3	2.7	0.3
1 Walnut SBT 90s	55.0	0.9	0.2	0.0
2 Watts SBT 90s	137.7	2.2	0.4	0.1
3 Maple SBT 90s	117.6	2.4	1.0	0.1
4 Colombia SBT 90s	271.8	6.5	2.3	0.4
5 Crown SBT 90s	170.7	6.2	2.3	0.2
1 Walnut SBT 100s	50.4	0.5	0.1	0.0
2 Watts SBT 100s	97.2	0.8	0.2	0.0
3 Maple SBT 100s	88.0	1.7	0.5	0.1
4 Colombia SBT 100s	316.9	9.6	4.7	0.5
5 Crown SBT 100s	161.9	6.2	1.9	0.2
1 Walnut SBT 110s	75.9	1.5	0.5	0.1
2 Watts SBT 110s	97.8	0.9	0.2	0.0
3 Maple SBT 110s	85.5	1.6	0.4	0.1
4 Colombia SBT 110s	295.6	6.7	3.1	0.4
5 Crown SBT 110s	192.8	5.4	1.8	0.2

Table 31. SBL Performance at Shorter Cycle Lengths

Row Labels	Queue Length	Vehicle Delay	Stop Delay	Stops
1 Walnut SBL 70s	74.3	23.2	13.9	1.3
3 Maple SBL 70s	48.2	26.1	17.0	0.9
4 Colombia SBL 70s	28.0	32.4	23.6	1.0
5 Crown SBL 70s	86.8	38.0	26.7	0.9
1 Walnut SBL 80s	83.1	25.7	15.8	1.3
3 Maple SBL 80s	44.0	23.3	14.8	0.8
4 Colombia SBL 80s	34.7	36.3	27.4	1.0
5 Crown SBL 80s	100.4	48.3	36.4	1.0
1 Walnut SBL 90s	67.5	19.3	11.2	1.0
3 Maple SBL 90s	50.5	13.0	6.1	0.7
4 Colombia SBL 90s	19.1	25.2	17.7	0.9
5 Crown SBL 90s	102.0	58.8	46.1	1.1
1 Walnut SBL 100s	66.4	19.6	11.5	1.0
3 Maple SBL 100s	62.2	12.1	5.4	0.7
4 Colombia SBL 100s	26.8	19.4	11.0	0.8
5 Crown SBL 100s	99.0	67.4	54.3	1.1
1 Walnut SBL 110s	108.3	28.7	18.7	1.3
3 Maple SBL 110s	58.1	15.3	8.0	0.8
4 Colombia SBL 110s	16.8	15.2	8.2	0.7
5 Crown SBL 110s	129.7	119.5	102.9	1.6

Table 32. SBR Performance at Shorter Cycle Lengths

Row Labels	Queue Length	Vehicle Delay	Stop Delay	Stops
1 Walnut SBR 70s	69.8	0.7	0.1	0.0
2 Watts SBR 70s	130.0	1.1	0.3	0.1
3 Maple SBR 70s	310.4	8.5	1.5	0.6
4 Colombia SBR 70s	107.8	3.4	0.4	0.1
5 Crown SBR 70s	45.3	5.6	0.1	0.5
1 Walnut SBR 80s	80.5	0.5	0.0	0.0
2 Watts SBR 80s	106.0	0.9	0.2	0.0
3 Maple SBR 80s	331.9	9.3	2.2	0.6
4 Colombia SBR 80s	260.7	4.9	0.3	0.2
5 Crown SBR 80s	37.0	4.2	0.0	0.3
1 Walnut SBR 90s	80.3	0.7	0.0	0.0
2 Watts SBR 90s	154.9	1.7	0.4	0.1
3 Maple SBR 90s	131.0	2.5	0.4	0.2
4 Colombia SBR 90s	287.1	6.8	1.9	0.4
5 Crown SBR 90s	39.5	4.1	0.0	0.3
1 Walnut SBR 100s	75.7	0.7	0.1	0.0
2 Watts SBR 100s	114.4	1.5	0.4	0.1
3 Maple SBR 100s	101.4	0.6	0.1	0.0
4 Colombia SBR 100s	332.3	10.3	4.5	0.5
5 Crown SBR 100s	23.1	2.4	0.0	0.1
1 Walnut SBR 110s	101.2	0.7	0.0	0.0
2 Watts SBR 110s	115.1	1.2	0.2	0.1
3 Maple SBR 110s	98.9	1.4	0.4	0.1
4 Colombia SBR 110s	311.0	7.1	2.5	0.4
5 Crown SBR 110s	28.5	2.6	0.0	0.1

Table 33. EBT Performance at Shorter Cycle Lengths

Row Labels	Queue Length	Vehicle Delay	Stop Delay	Stops
1 Walnut EBT 70s	45.5	30.0	23.8	0.9
3 Maple EBT 70s	92.8	37.1	29.8	1.0
5 Crown EBT 70s	28.9	32.6	23.4	0.8
1 Walnut EBT 80s	53.8	36.2	29.2	0.9
3 Maple EBT 80s	94.1	39.8	33.1	0.9
5 Crown EBT 80s	30.8	34.9	25.5	0.8
1 Walnut EBT 90s	53.5	34.6	28.2	1.1
3 Maple EBT 90s	118.4	54.1	46.0	1.1
5 Crown EBT 90s	32.7	51.7	41.7	1.0
1 Walnut EBT 100s	65.8	40.8	33.2	1.7
3 Maple EBT 100s	120.2	60.1	52.3	1.0
5 Crown EBT 100s	32.5	42.9	33.3	0.9
1 Walnut EBT 110s	66.3	48.6	41.2	1.5
3 Maple EBT 110s	126.2	65.9	57.4	1.1
5 Crown EBT 110s	29.7	59.3	48.7	1.0

Table 34. EBL Performance at Shorter Cycle Lengths

Row Labels	Queue Length	Vehicle Delay	Stop Delay	Stops
1 Walnut EBL 70s	45.5	28.2	20.0	1.0
2 Watts EBL 70s	221.4	76.7	64.0	1.7
3 Maple EBL 70s	92.8	31.5	24.2	0.9
5 Crown EBL 70s	34.4	22.4	16.9	0.6
1 Walnut EBL 80s	53.8	31.3	22.9	1.0
2 Watts EBL 80s	353.4	252.0	152.2	3.0
3 Maple EBL 80s	94.1	48.2	33.6	0.9
5 Crown EBL 80s	33.2	27.5	24.8	0.8
1 Walnut EBL 90s	53.5	43.7	31.2	1.3
2 Watts EBL 90s	362.9	188.4	162.3	2.9
3 Maple EBL 90s	118.4	49.9	47.2	1.1
5 Crown EBL 90s	36.4	33.4	27.9	0.9
1 Walnut EBL 100s	65.8	45.0	41.3	1.4
2 Watts EBL 100s	576.1	424.7	359.1	5.0
3 Maple EBL 100s	120.2	67.6	53.3	1.1
5 Crown EBL 100s	40.0	40.7	32.3	0.8
1 Walnut EBL 110s	66.3	55.6	45.4	1.4
2 Watts EBL 110s	580.0	459.7	434.4	5.6
3 Maple EBL 110s	126.2	72.2	61.2	1.2
5 Crown EBL 110s	40.2	46.7	30.4	0.8

Table 35. EBR Performance at Shorter Cycle Lengths

Row Labels	Queue Length	Vehicle Delay	Stop Delay	Stops
1 Walnut EBR 70s	44.2	9.1	0.8	1.0
2 Watts EBR 70s	114.1	37.7	14.6	1.7
3 Maple EBR 70s	45.3	9.7	1.8	1.1
5 Crown EBR 70s	88.9	11.0	0.4	0.9
1 Walnut EBR 80s	44.9	8.7	0.8	1.2
2 Watts EBR 80s	246.6	178.4	78.3	3.3
3 Maple EBR 80s	45.5	9.5	1.7	1.1
5 Crown EBR 80s	86.4	10.8	0.4	1.0
1 Walnut EBR 90s	44.7	8.8	1.2	1.0
2 Watts EBR 90s	236.3	127.7	92.1	3.3
3 Maple EBR 90s	48.0	10.3	3.2	1.2
5 Crown EBR 90s	88.0	10.7	0.3	0.9
1 Walnut EBR 100s	38.7	8.9	0.4	0.9
2 Watts EBR 100s	592.6	302.6	252.9	4.9
3 Maple EBR 100s	48.7	11.9	1.6	1.2
5 Crown EBR 100s	98.8	11.6	0.3	1.0
1 Walnut EBR 110s	51.4	9.3	0.7	1.0
2 Watts EBR 110s	596.5	343.7	302.7	5.4
3 Maple EBR 110s	42.1	16.2	1.8	1.2
5 Crown EBR 110s	98.8	11.5	0.4	1.0

Table 36. WBT Performance at Shorter Cycle Lengths

Row Labels	Queue Length	Vehicle Delay	Stop Delay	Stops
1 Walnut WBT 70s	58.6	29.8	24.7	1.0
3 Maple WBT 70s	62.9	18.6	10.0	1.6
4 Colombia WBT 70s	72.6	30.4	24.3	0.8
5 Crown WBT 70s	77.6	42.7	31.9	1.2
1 Walnut WBT 80s	58.4	38.7	33.7	0.9
3 Maple WBT 80s	58.4	18.7	11.2	1.6
4 Colombia WBT 80s	87.6	34.7	28.5	0.9
5 Crown WBT 80s	74.3	41.5	31.4	1.0
1 Walnut WBT 90s	63.4	22.2	18.0	0.9
3 Maple WBT 90s	58.3	21.0	13.4	1.6
4 Colombia WBT 90s	88.1	43.1	36.5	1.0
5 Crown WBT 90s	86.0	50.6	39.4	1.2
1 Walnut WBT 100s	57.2	49.3	43.8	1.2
3 Maple WBT 100s	57.3	15.3	7.4	1.7
4 Colombia WBT 100s	92.4	50.8	43.2	1.1
5 Crown WBT 100s	71.1	49.6	40.5	1.0
1 Walnut WBT 110s	73.5	50.5	45.4	1.0
3 Maple WBT 110s	61.7	16.5	8.9	1.5
4 Colombia WBT 110s	116.1	81.5	70.0	1.6
5 Crown WBT 110s	76.7	43.6	33.2	1.1

Table 37. WBL Performance at Shorter Cycle Lengths

Row Labels	Queue Length	Vehicle Delay	Stop Delay	Stops
1 Walnut WBL 70s	58.6	25.8	20.7	0.9
3 Maple WBL 70s	68.6	32.0	26.9	0.9
4 Colombia WBL 70s	119.4	41.2	34.1	1.0
5 Crown WBL 70s	100.3	27.3	14.5	1.7
1 Walnut WBL 80s	58.4	32.8	27.6	0.9
3 Maple WBL 80s	64.4	38.9	33.6	0.9
4 Colombia WBL 80s	127.8	50.6	43.1	1.1
5 Crown WBL 80s	97.0	26.4	13.8	1.7
1 Walnut WBL 90s	63.4	36.9	31.4	1.1
3 Maple WBL 90s	69.6	43.6	38.2	1.0
4 Colombia WBL 90s	140.0	62.1	53.9	1.2
5 Crown WBL 90s	108.7	31.9	18.2	1.8
1 Walnut WBL 100s	57.2	43.1	37.4	1.1
3 Maple WBL 100s	64.8	46.7	41.7	0.9
4 Colombia WBL 100s	218.5	106.0	94.4	1.6
5 Crown WBL 100s	93.9	30.3	17.2	1.8
1 Walnut WBL 110s	73.5	43.2	37.5	1.1
3 Maple WBL 110s	81.4	60.3	54.5	1.0
4 Colombia WBL 110s	226.8	143.0	129.1	2.0
5 Crown WBL 110s	99.4	32.1	19.3	1.7

Table 38. WBR Performance at Shorter Cycle Lengths

Row Labels	Queue Length	Vehicle Delay	Stop Delay	Stops
1 Walnut WBR 70s	61.1	13.2	5.1	1.6
3 Maple WBR 70s	61.7	16.5	9.0	1.5
4 Colombia WBR 70s	99.4	23.9	14.8	1.4
5 Crown WBR 70s	53.6	30.9	22.5	0.8
1 Walnut WBR 80s	62.6	13.2	5.0	1.5
3 Maple WBR 80s	57.3	15.6	8.2	1.4
4 Colombia WBR 80s	114.3	26.0	16.8	1.5
5 Crown WBR 80s	56.4	34.0	25.4	0.8
1 Walnut WBR 90s	59.3	9.8	3.0	1.2
3 Maple WBR 90s	57.1	14.8	7.8	1.4
4 Colombia WBR 90s	114.9	24.7	15.0	1.5
5 Crown WBR 90s	57.9	32.1	23.3	0.8
1 Walnut WBR 100s	62.9	11.6	3.6	1.5
3 Maple WBR 100s	56.2	13.5	6.3	1.5
4 Colombia WBR 100s	119.1	35.3	23.4	1.8
5 Crown WBR 100s	62.6	42.4	33.5	0.9
1 Walnut WBR 110s	66.5	11.8	4.6	1.4
3 Maple WBR 110s	60.6	13.8	6.1	1.5
4 Colombia WBR 110s	142.8	54.8	41.2	2.1
5 Crown WBR 110s	66.1	44.5	35.6	0.9

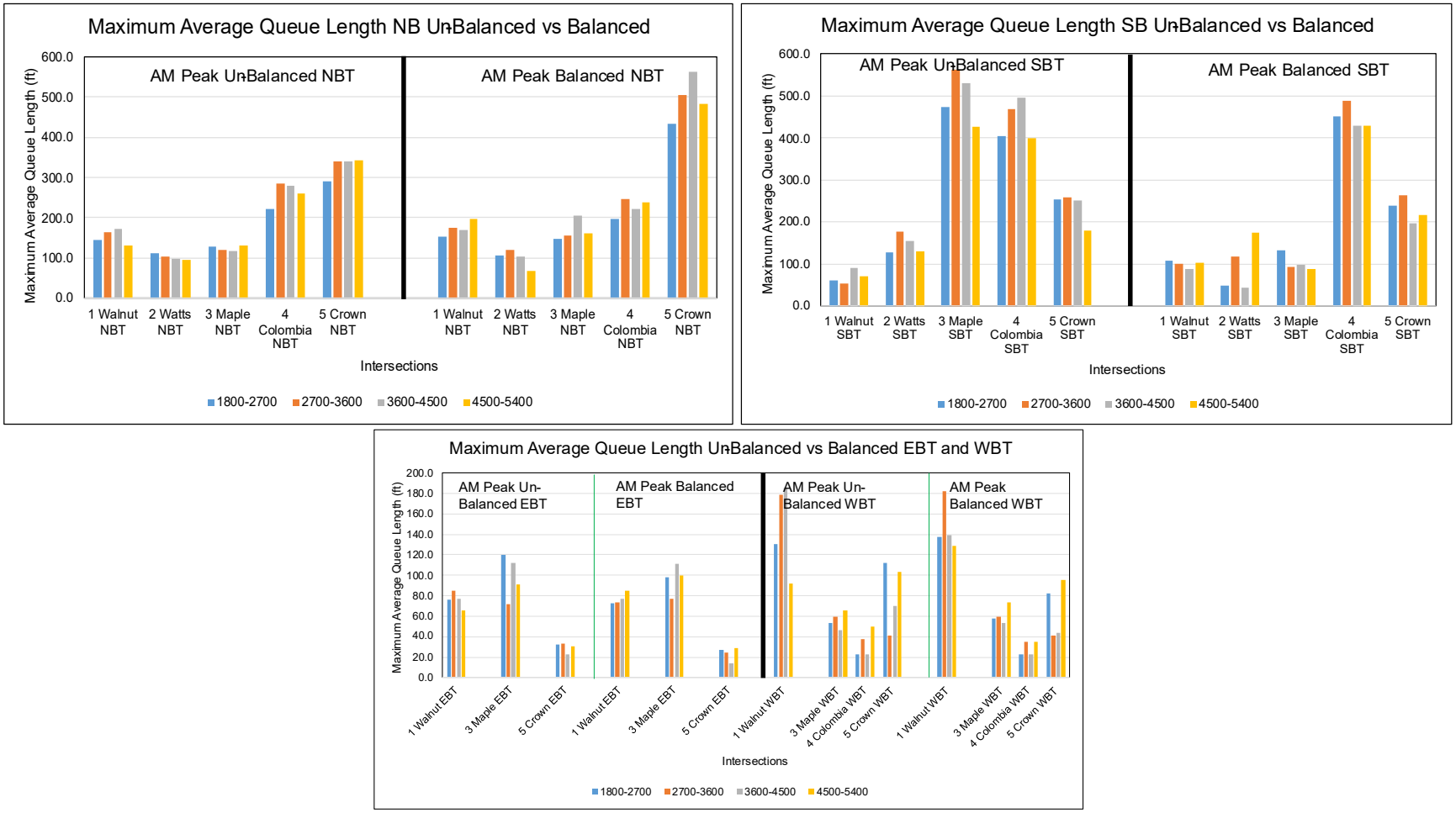

Figure 32. Average Queue Lengths AM-Peak

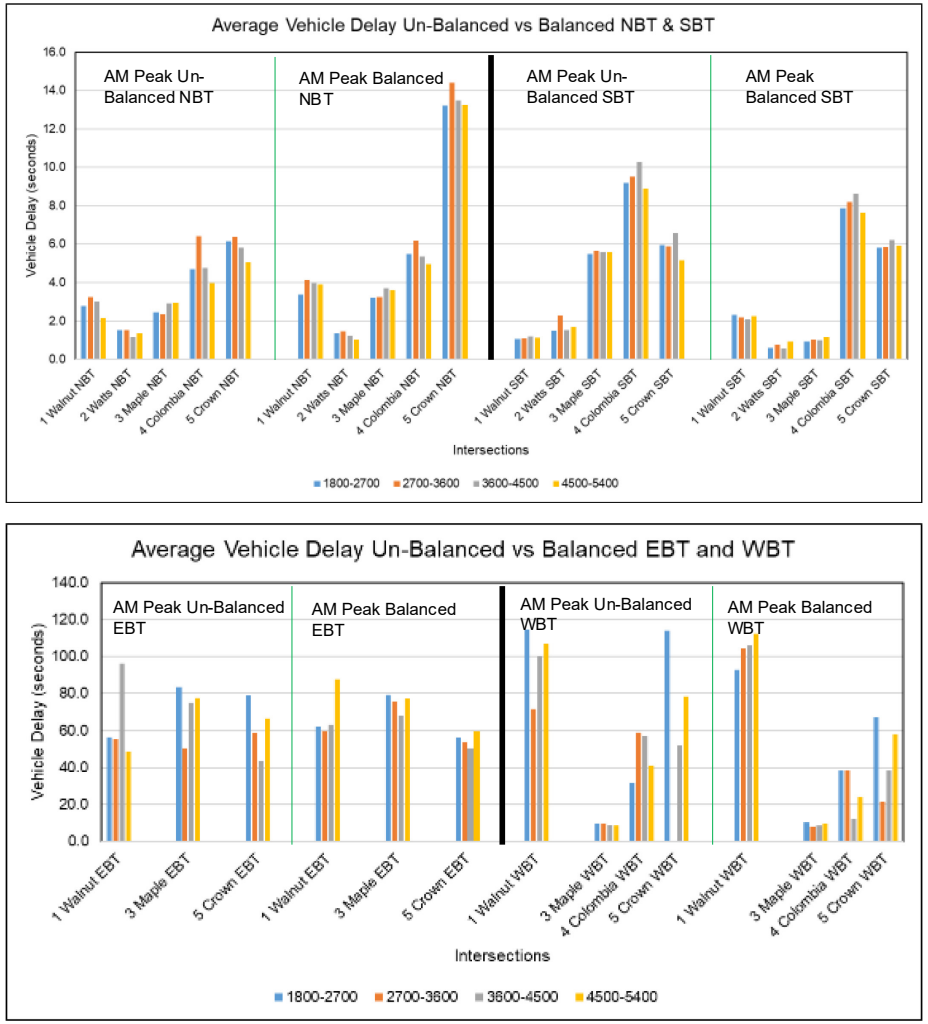

Figure 33. Average Vehicle Delay During AM-Peak

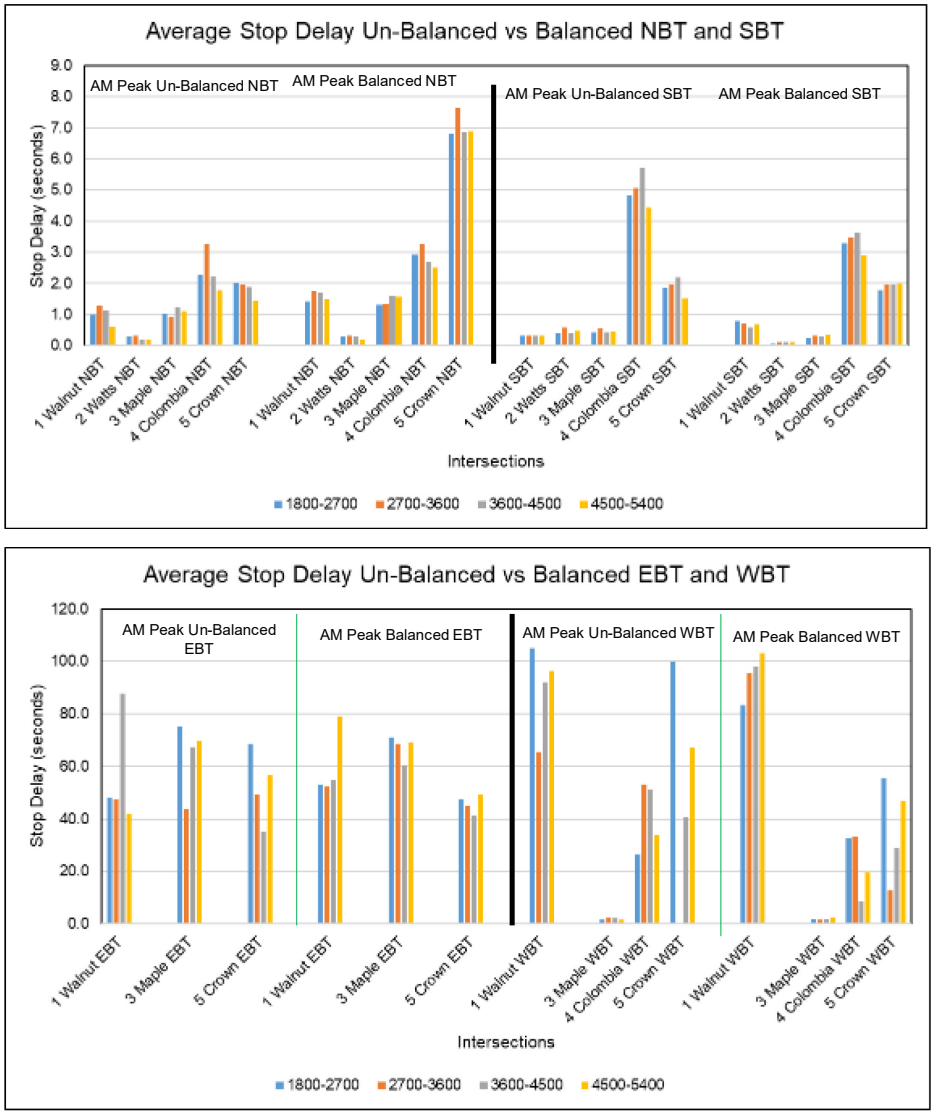

Figure 34. Average Stop Delay AM-Peak

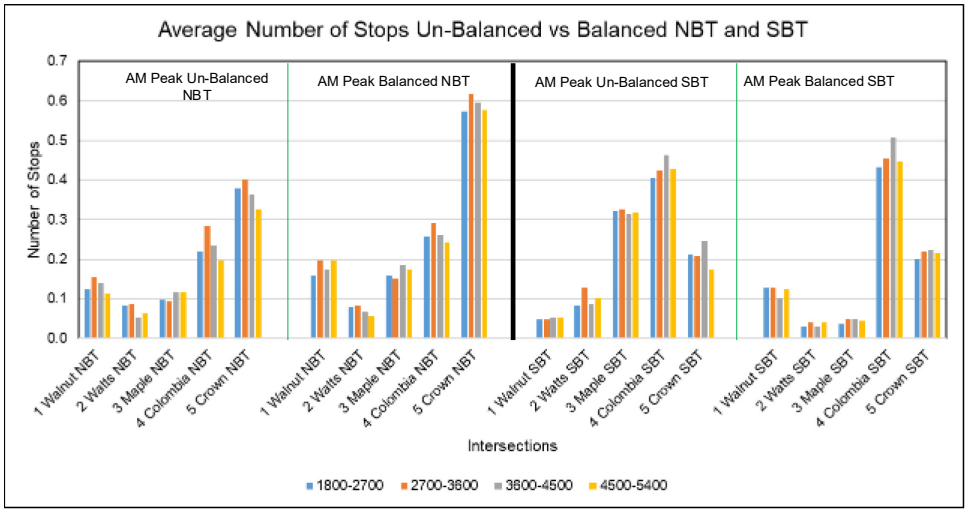

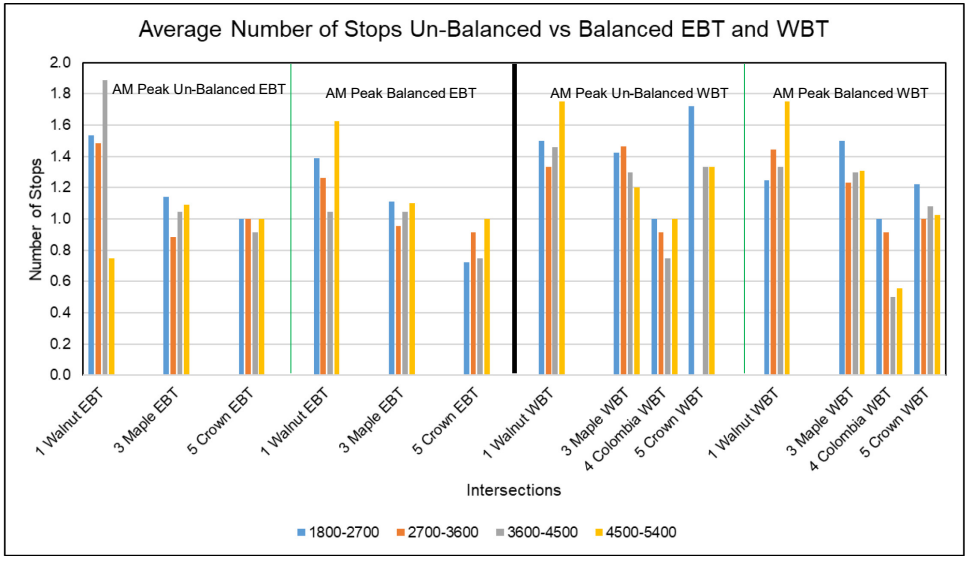

Figure 35. Average Number of Stops AM-Peak

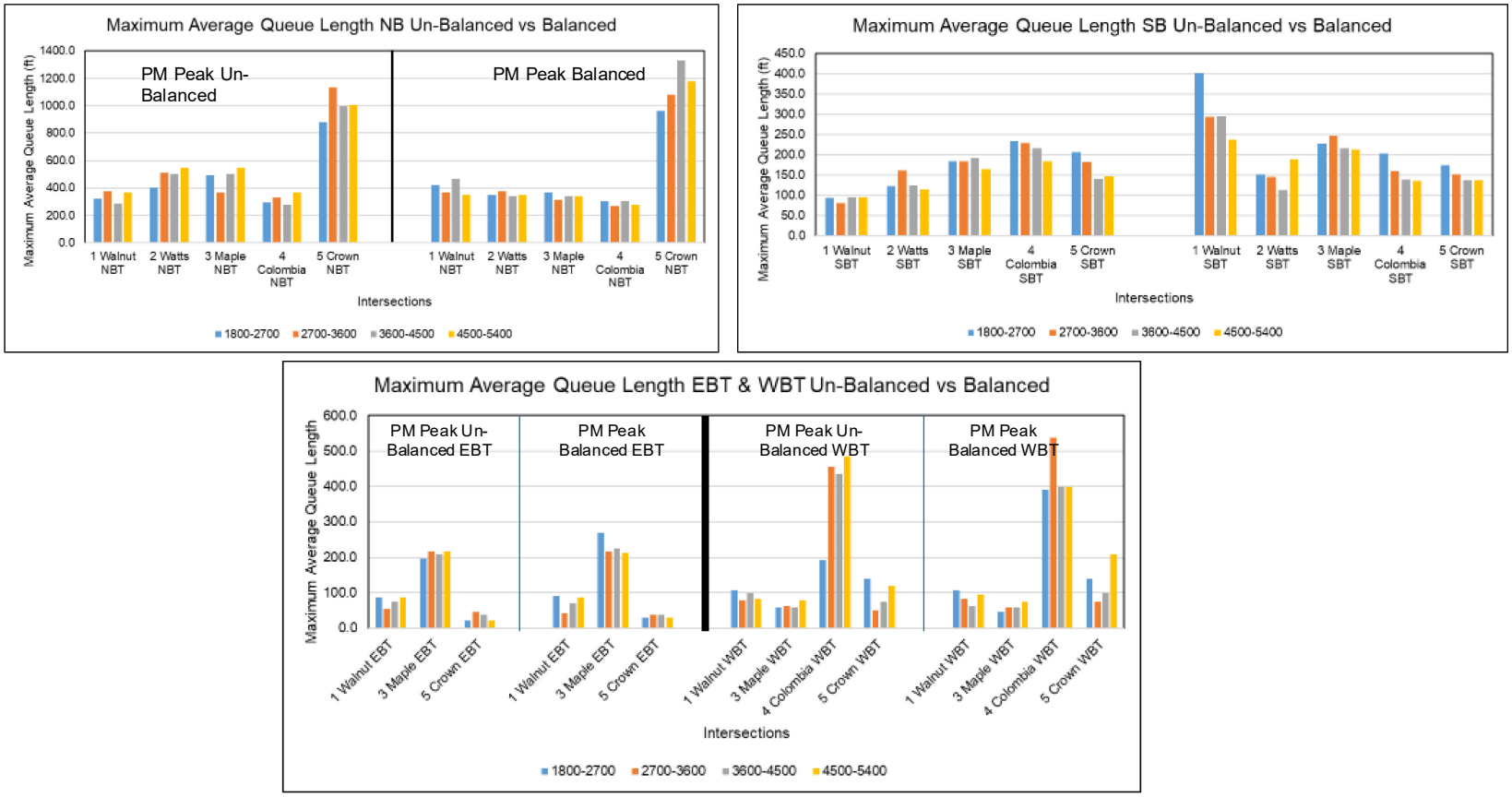

Figure 36. Average Queue Length PM-Peak

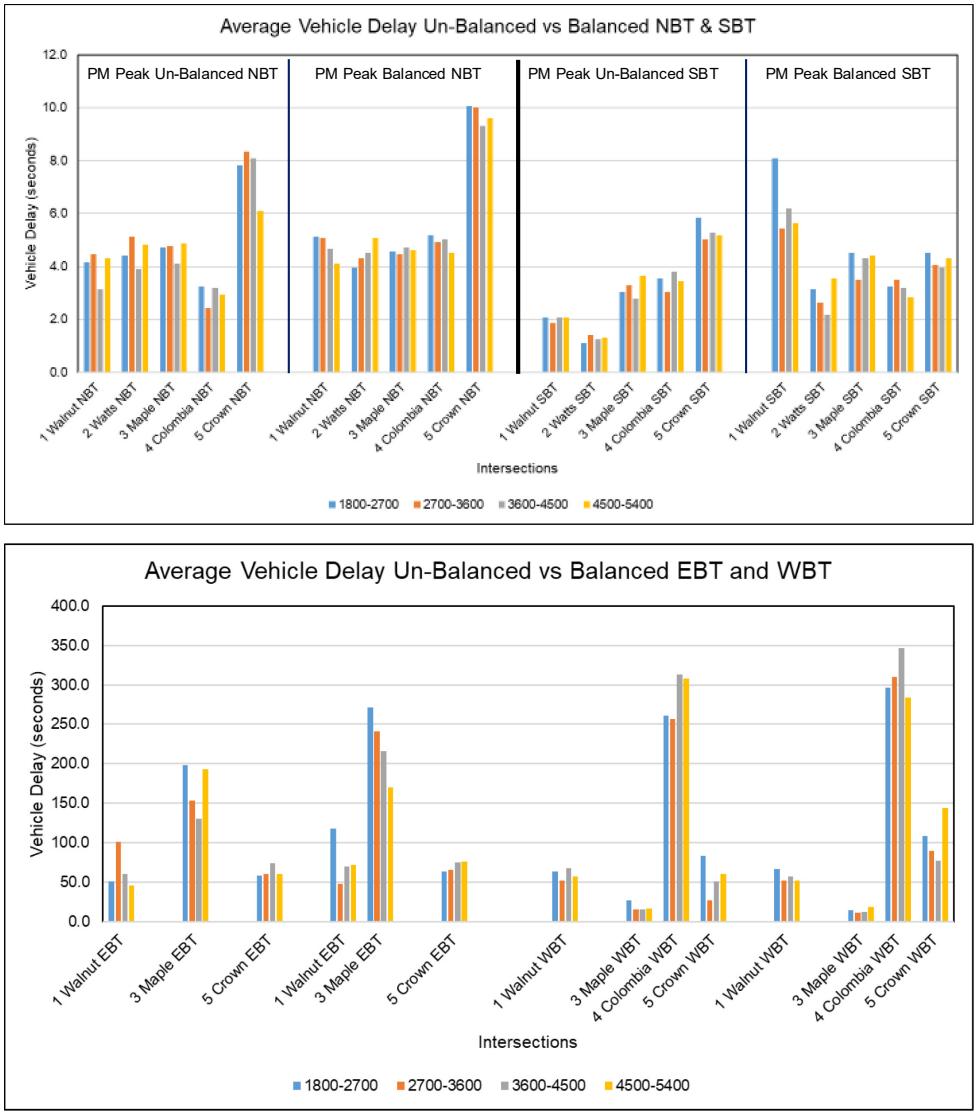

Figure 37. Average Vehicle Delay PM-Peak

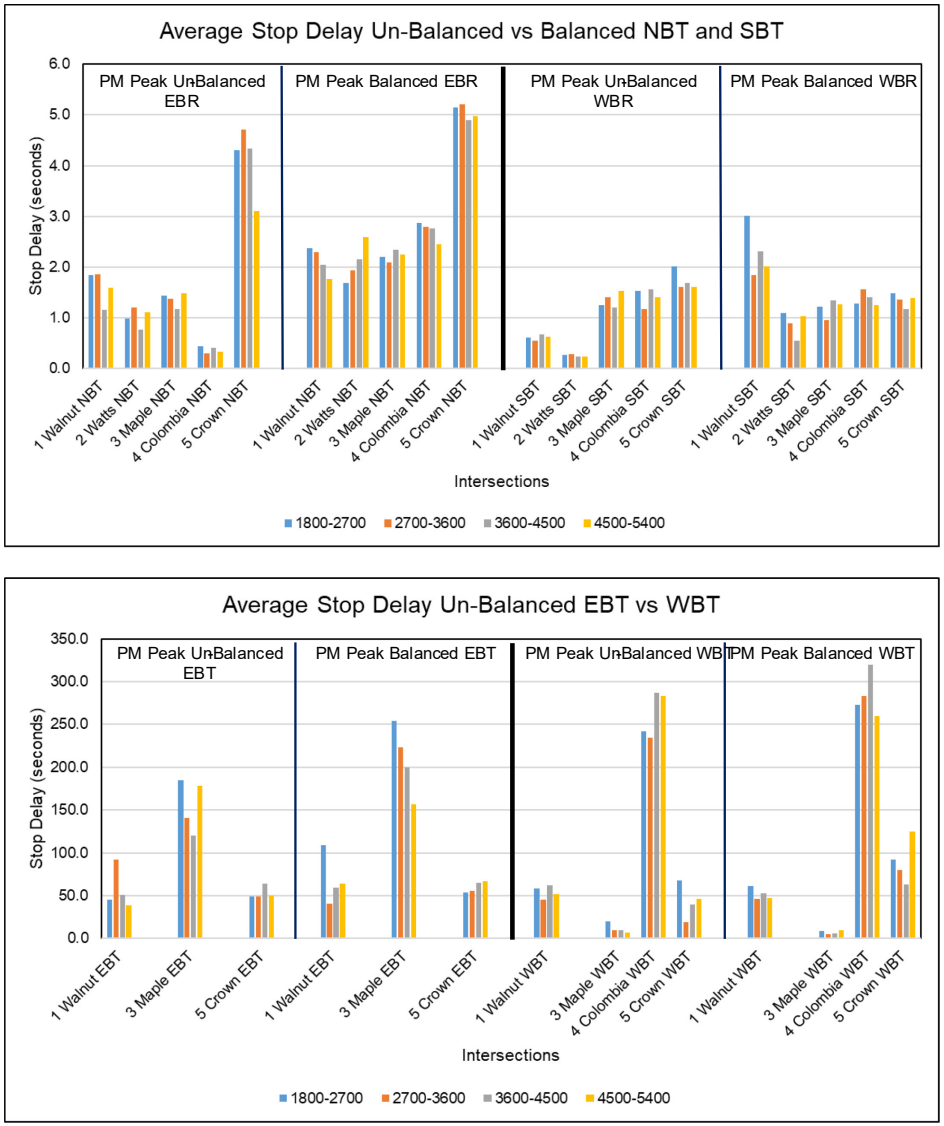

Figure 38. Average Stop Delay PM-Peak

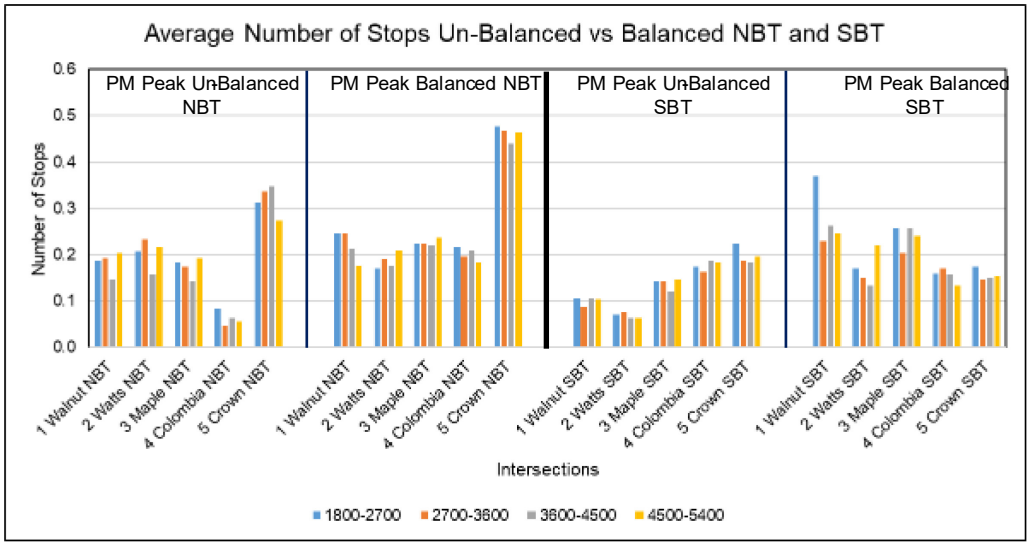

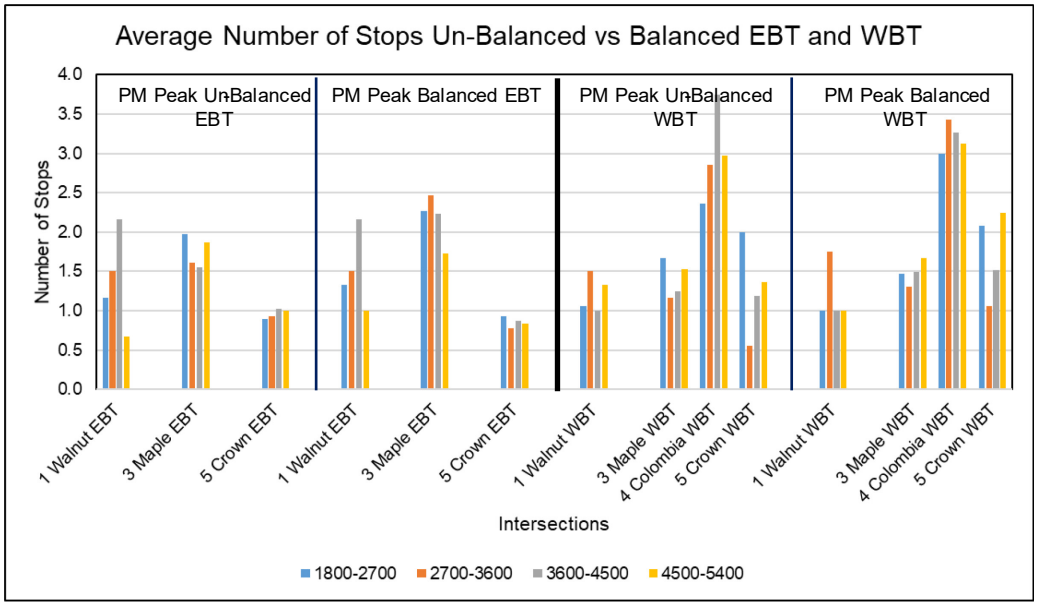

Figure 39. Average Number of Stop PM-Peak